Rejuvenation driven reprograming in T lymphocytes

Alessio Lanna

alessio.lanna@sentcell.life

Sentcell https://orcid.org/0000-0003-2215-3748

Clara D'Ambra

Sentcell

Manuel Delpero

MGI

Melania Capitani

Sentcell

Luisa Chocarro

Pamplona University

Federica Rinaldi

Sentcell

Michael Karin

UCSD

Letter

Keywords:

Posted Date: October 10th, 2024

DOI: https://doi.org/10.21203/rs.3.rs-5180379/v1

Additional Declarations: Yes there is potential Competing Interest. A.L. is a shareholder to Sentcell ltd and the sole inventor of the DOS pharmaceutics where Sentcell ltd figures as the Applicant (PCT/IT2021/000059). M.K. serves as a scientific advisor to Sentcell ltd. A.L. M.C and F.R. are supported by Sentcell ltd.

Rejuvenation driven reprograming in T lymphocytes

Alessio Lanna[1,2,*], Clara D'Ambra[1], Manuel Delpero[3], Melania Capitani[1], Luisa Chocarro[4], Federica Rinaldi[1] & Michael Karin[5]

[1] Sentcell UK laboratories, Tuscany Life Sciences, GSK Vaccine Campus, Siena. Italy

[2]University College London, Division of Medicine, London. United Kingdom.

[3]Humboldt-Universität zu Berlin, Berlin. Germany

[4]Oncoimmunology Unit, Navarrabiomed, Fundación Miguel Servet, Universidad Pública de Navarra Pamplona, Spain.

[5] University of California San Diego, San Diego. USA.

*Correspondence to:

Prof. Dr. Alessio Lanna

Email: **alessio.lanna@sentcell.life**

Abstract

Rejuvenation restores cellular function lost with age, but it is not known to confer properties the cell lacked in its younger past. We found that Disruptors of sestrin-MAPK interactions (DOS) reprogramed senescent T cells into new stem like T clones with different T cell receptors (TCRs). DOS targeted sestrin-MAPK complexes (sMAC) to ubiquitin-dependent proteasomal degradation, resulting in long-term sestrin transcriptional inhibition, increased T cell fitness, and generation of long-lived stem like memory clones. Strikingly, DOS reactivated juvenile related Rag re-expression, leading to antigen-specific TCR rearrangements in formerly senescent cells. As such, rejuvenated T cells, with stem features and new TCRs, combated multiple lethal challenges never previously encountered in their lifetime, with no need for vaccination. T cell rejuvenation confers new properties whilst preserving cellular state, which unravels an unknown rejuvenating principle in biological systems.

Cellular functions deteriorate during aging[1-3] and several attempts at rejuvenating or reprograming somatic cells have been proposed. Somatic cells may be reverted to pluripotency and converted to a desired cell type via de-differentiation/re-differentiation cycles with specific transcription factors[4,5]. Alternatively, partial reprograming can avoid de-differentiation and restore more efficient cellular functions, overlapping those previously displayed at younger age[6-8]. Trans-differentiation has also been employed to convert adult immune cell types bypassing any intermediate stem stage[9]. Further work had shown that certain exhausted T cells could be reinvigorated upon somatic reprograming[10,11] but failed to generate different immune repertoires. Whether rejuvenation may confer new functions preserving cell state is not known.

To explore functional gains associated with rejuvenation, we targeted T cells in which aging phenotypes are imposed by stress interactions of sestrins activating AMPK in a complex with MAPKs

(sMACs)[12-14]. We designed simple *in vitro* assays composed of recombinant sestrin and AMPK incubated with 156 pentameric sestrin peptides that may disrupt an interaction between the two proteins (**Extended Data Fig. 1a-c**). Upon peptide cyclisation, we identified the disruptor of sMAC (DOS) 46L, the lead compound (**Fig. 1a** and **Extended Data Fig. 1d**). Using Autodocking with an AlphaFold algorithm[15], DOS46L was predicted to bind to sestrins in a site that is distal to that required for GATOR/mTOR regulation[16] (**Fig. 1b** Site 1 and **Extended Data Fig. 2a**). Site directed sestrin 2 mutagenesis in primary T cells confirmed docking predictions (**Extended Data Fig. 2b, c**). *In vitro* assays further showed direct DOS binding to recombinant sestrins, resulting in AMPK inactivation (**Fig. 1c-e**).

In culture, DOS selectively penetrated the $sMAC^+$ T cells within minutes of treatment (**Fig. 1f**), especially immune senescent $CD27^-$ $CD28^-$ $CD4^+$ T cells (hereafter, T_{sen}) that possess the highest levels of sMACs[13] (**Extended Data Fig. 3a**). By contrast, DOS did not enter sestrin deficient T cells (**Fig. 1f**). Imaging studies confirmed intracellular DOS penetrance in activated $CD4^+$ T cells (**Fig. 1g**). DOS did not alter the extent of CD4 internalization upon TCR activation (**Extended Data Fig. 3b**), and colocalized to the ER where the sMAC resides (**Extended Data Fig. 3c**). Correspondingly, DOS bound to the sMAC but no other sestrin complexes containing GATOR/mTOR proteins[17] (MIOS and WDR59; **Fig. 1h**). As expected, T_{sen} sMAC suppression by DOS required AMPK (sestrin-bound MAPK activities; **Fig. 1i** and **Extended Data Fig. 3d, e**). Upon intracellular binding, DOS triggered sestrin-AMPK dissociation (**Extended Data Fig. 3f**) and subsequent ubiquitin mediated proteasome degradation (**Fig. 1h-k** and **Extended Data Fig. 3g**), resulting in sestrin downregulation, and AMPK inactivation in T_{sen} (**Fig. 1l** and **Extended Data Fig. 3h**). DOS also inhibited sMACs in senescent human $CD8^+$ T cells (**Extended Data Fig. 3i**), and upon irradiation induced senescence (**Extended Data Fig. 3j**).

AMPK is inhibited when ATP binds to cystathionine β-synthetase (CBS) sites within its gamma subunit[18,19] (**Extended Data Fig. 4e**). Studying how sMAC dismantling could be initiated, we found that DOS opposed sestrin action on AMPK-γ almost instantaneously, enforcing ATP levels in response to sestrin treatment (**Extended Data Fig. 4a-c**), and could be counteracted by an allosteric AMPK activator (A-769662) that operates better when AMPK is ATP bound[20] (**Extended Data Fig. 4d**). Similar results with a fluorescent analogue of ATP which specifically binds to the CBS1/3 sites[18-19] (**Extended Data Fig. 4e**). Because activated AMPK had more sestrin binding affinity than inactive AMPK (**Extended Data Fig. 4f**), the data showed that once inhibited at the point of its adenosine exchanging sites, inactive AMPK loses sestrin affinity (**Extended Data Fig. 4g**), and sMAC degradation begins (**Extended Data Fig. 4h**).

When we derived $sMAC^+$ vs $sMAC^-$ T cells by activated single cell sorting[21,22] (**Extended Data Fig. 5a**), we found that only $sMAC^+$ T cells could be subjected to rejuvenation, as demonstrated by enhanced DOS-driven Fatty Acid Oxidation (FAO) in Seahorse assessments (**Extended Data Fig. 5b**). We reasoned that DOS may have induced juvenile related beta-catenin activity among $sMAC^+$ T cells, because this protein activates FAO related transcription[23,24]. In fact, DOS unleashed beta-catenin from p53 inhibitory binding[25,26] among $sMAC^+$ T cells (**Extended Data Fig. 5c**), thereby promoting juvenile related transcription programs, as shown in both Chip (**Extended Data Fig. 5d**) and luciferase reporter assays (**Extended Data Fig. 5e**). Importantly, DOS-driven beta-catenin reactivation also resulted in stem-like induction (**Extended Data Fig. 5f**), unless drugs that interfere with beta catenin mediated transcription were used (**Extended Data Fig. 5d-f**). DOS unleashes juvenile related programs in $sMAC^+$ T cells (**Extended Data Fig. 5g**).

Because sMAC is most abundant in senescent T cells[13], we assessed the juvenile state induced by DOS in reverting the senescence state as well the expression of established senescence markers[27]. We found reversal of expression of β-galactosidase (**Fig. 2a**) and DNA damage associated foci (**Extended Data**

Fig. 6a) in human T_{sen}, activated in the presence of DOS for one week, as well restored T_{sen} proliferation in culture (**Fig. 2b, left**). The proliferative boost was sestrin dependent (triple shRNAs; **Fig. 2b, right**).

Restored proliferation was also documented with a cell dilution assay (Cell Trace Violet (CTV), **Extended Data Fig. 6b**) or bromodeoxyuridine (BrdU) incorporation (**Extended Data Fig. 6c**). Cell cycle progression, increased in cyclins and decreased in cell cycle suppressors occurred (**Extended Data Fig. 6d, e**). We also genetically silenced AMPK in long term T_{sen} cultures, with analogue results (**Extended Data Fig. 6f**).

Strikingly, DOS converted highly purified senescent effector memory $CD27^-$ $CD28^-$ $CD4^+$ T cells that lack CD45RA expression ($senT_{EM}$) (**Extended Data Fig. 6g**) to a $CD45RA^+$ $CD28^+$ $CD62L^+$ $CD95^+$ $TCF1^+$ $CD4^+$ stem like memory state[28]. Stem like switches kept growing, steadily, throughout the 21-day culture (**Fig. 2c**). In these experiments, DOS-induced stem generation occurs through intermediate CD45RA restoration (T_{EMRA} stage) followed by complete stem-like conversion (**Fig. 2c**). By contrast, DOS had no effect on truly naïve T cell frequencies or nonsenescent T cell effectors that lack sMACs (**Extended Data Fig. 6h**). Senescent T cell rejuvenation manifests as stem like T cell reprograming (DOS-juvenation (DOS_{juv})). Furthermore, DOS_{juv} T cells demonstrated improved cell behaviour (**Extended Data Fig. 6i-l**). Telomerase activity was not affected (**Extended Data Fig. 6m**). No cell damage or death (**Extended Data Fig. 6n**).

An adoptive transfer system, with congenic surface tracking or Cell Trace Violet (CTV) labelling[29], demonstrated that DOS_{juv} T cell reprograming restored old T cell lifespan in vivo (**Fig. 2d, e**). In mice, DOS_{juv} T cells also switched to a $CD44^-$ $CD62L^+$ $CD95^+$ stem like memory state, with reduced numbers of $CD44^-$ $CD62L^-$ terminal effectors (TE) among the CD45.1 transferred $CD4^+$ T cells *in vivo* (**Fig. 2f**). Central (but not effector) memory $CD4^+$ T cell phenotypes were also enhanced (**Extended**

Data Fig. 7). There was also restoration of IL7-receptor transcripts (**Fig. 2g**) and further stem like memory marker expression among the DOS-transferred T cells (**Fig. 2h**). DOS responses mirrored those of young $CD4^+$ T cell transfer (**Fig. 2d-h**). When transferred, most donor cells lacked expression of the cell cycle related Ki67 nuclear antigen and persisted in this resting state 28 days after transfer (**Fig. 2i, j**). Importantly, in the absence of DOS, old transferred T cells largely died due to necrosis (PI^+ Annexin- T cells; **Fig. 2k**). Similar results were obtained with CTV labelling (**Extended Data Fig. 8**). T cell reprograming generates long-lived, stem-like memory cells that are largely quiescent in vivo (**Fig. 2l**).

In further experiments (**Extended Data Fig. 9a**), DOS_{juv} ($CD4^+$) T cell transfer restored isotopic switched $CD38^+$ $CD19^+$ IgG^+ memory B cell generation[30,31] among lymph nodes of old vaccinated recipients (Fluad; **Extended Data Fig. 9b**). Correspondingly, flu-specific immunoglobulines (IgG1s) were restored by the DOS_{juv} T cells (**Extended Data Fig. 9c**). These results phenocopied transfer-free animals, when assessing young or DOS-treated mice subjected to vaccination (**Extended Data Fig. 9b,c**); and human immune cultures from aged individuals, where DOS restored Fluad-specific IgG production via the $CD4^+$ T cells (**Extended Data Fig. 9d**). Further phenotypic switches that support humoral responses[32,33] were also detected (**Extended Data Fig. 10a, b**), and in a $CD4^+$ T cell sestrin dependent way (**Extended Data Fig. 10c,d**). Therefore, $CD4^+$ T cells are essential for DOS action, suggesting these T cells would confer immune protection upon vaccination.

However, we found that DOS_{juv} T cells greatly protected old recipients from a lethal flu infection even in the absence of vaccination (**Fig. 3a, b**). By contrast, old recipient animals without DOS_{juv} T cell transfer largely succumbed to the infection despite vaccination. DOS_{juv} T cells triggered H1N1 viral specific antibody production (**Fig. 3c**), with neutralising activity (Micro-neutralisation assays with MDCK cells; **Fig. 3d**) and eradication of viral titres in vivo (qPCR; **Fig. 3e**). DOS_{juv} T cells also induced antiviral Th1 cell responses in the infected lungs (**Fig. 3f, g**), well recognized events that

confer anti-viral protection and sterilizing immunity[34]. Moreover, flu-specific stem-like T cells were also observed among the DOS transferred T cells in the recipient organs (spleens; **Fig. 3h**). T cell rejuvenation had long lasting effects, as shown by long-term sestrin inhibition within the adoptively transferred DOS_{juv} T cells up to 6 months (**Fig. 3i**). Similar results were obtained by systemic DOS administration (**Extended Data Fig. 11**). T cell rejuvenation was also linked with reduced sestrin transcript and protein expression (**Extended Data Fig. 12a-d**), long-term deacetylation[35] of the sestrin gene (**Extended Data Fig. 12e**) and increased histone deacetylase activity (**Extended Data Fig. 12f**). DOS reprograms T cells, conferring long-term immune protection in a way that obviates any need for vaccination.

A vaccine-free protection was unexpected. Searching for a different mechanism of immune protection, we discovered increased levels of T cell receptor excision circles (TRECs)[36] among lymph nodes of flu infected, DOS treated animals (**Extended Data Fig. 13a**), as well expression of new TCRβ variants (**Extended Data Fig. 13b**). That suggested recent TCR rearrangements with new specificities[37]. Augmented TREC generation was also detected among DOS_{juv} T cells upon adoptive transfer (**Extended Data Fig. 13c**), some of which underwent negative selection *in vivo* (**Extended Data Fig. 13d**). No signs of autoimmunity were found during 2-year observations.

Similar TREC generation was observed in purified human T cells exposed to DOS treatment in culture (**Extended Data Fig. 13e**). These data suggest a new means for immune protection via T cell repertoire expansion.

Accordingly, DOS reprogramed T cells responded to antigens never previously encountered, such as yellow fever (YF), to which Western populations have not been exposed[38] (**Extended Data Fig. 13f**). These responses were exclusively evident among the human stem like compartment, which could not be simply explained by increased TCR sensitivity because T cells not exposed to the DOS never responded to YF, regardless of the antigen dosing (**Extended Data Fig. 13f**). Similar results in stem

like T cells isolated upon DOS-driven reprograming and analyzed by ELISA (**Extended Data Fig. 13g**) or using YF specific peptides, instead of a vaccine, in the immune-conjugate reactions (**Extended Data Fig. 13h, i**). DOS-driven YF specific responses were also evident among T cells derived from transgenic OT-II mice that express only an ovalbumin (OVA)-specific TCR (**Extended Data Fig. 13j**), further supporting generation of new TCRs. DOS-driven reprograming confers new TCR specificity.

Using next generation sequencing (NGS), we found rapid and specific TCR rearrangements among human T cells in culture with YF peptide loaded APCs (**Fig. 4a**), consisting of enhancement of TCR repertories and, strikingly, generation of new TCRs with antigen pockets that did not exist before DOS treatment (**Fig. 4b**). Individual TCR rearrangements were also detected in antigen-specific cultures where T cells had not been exposed to the DOS, yet to a much lower extent (**Extended Data Fig. 14a**). Importantly, generation of new antigen pockets largely required presence of DOS (**Fig 4b**), suggesting natural TCR revisions may not sufficiently shape antigen recognition in the absence of juvenile reprograming. Examination of TCR clonotypes revealed DOS-driven rearrangements exclusively amongst the rarest TCR β variants (**Extended Data Fig. 14b**), consistent with occurrence in rare antigen specific stem clones. In fact, DOS_{juv} T cells, expressed the NGS identified TCRs among the stem-like T cell compartment (**Fig. 4c**). Some senescent T_{EMRA} also showed new TCR variant expression, indicating TCR revision programs may begin early during DOS-driven reprograming, prior to stem like conversion (**Fig. 4c**). Dual TCR expressing T cells were not found (**Fig. 4c top right**).

Using CTV dilution assays, no trace of YF specific proliferation at this early assessment (18 hours; **Fig. 4d)**. However, DOS-treated, TRBV expressing T cells produced IFN-γ in response to YF activation at this time (**Fig. 4d, top right**), and demonstrated YF-specific activation in cytokine independent assays (**Fig. 4d, bottom right**). YF-specific responses were also confirmed in purified

202 TRBV expressing stem like T cell clones (**Fig. 4e, f**). Acquisition of new antigen-specific function is
203 strictly related to stem like T cell reprograming and precedes clonal expansion.
204
205 Testing how specific rearrangements occurred, we found DOS induction of Rag 1 and 2 proteins in
206 peripheral $CD4^+$ T cells (**Fig. 5a**) that mediate TCR recombination in the thymus but have naturally
207 low expression in mature T cell populations[39,40]. Moreover, Rag proteins were bound to the T cell
208 DNA (**Fig. 5b**). Strikingly, Rag re-expression was due to beta catenin mediated transcription unleashed
209 by the DOS (**Fig. 5c, d**).
210
211 To link T cell reprograming with new immune specific activation, we measured the phosphorylation
212 status of LCK[41], an essential TCR signalling enzyme that is recruited at the onset of the antigen specific
213 response. We found early evidence of YF-specific TCR activation, exclusively among those TEMRA
214 that firstly arise from senescence during reprograming (**Fig. 2c**), and that had down-regulated their
215 CD3 as part of the TCR revisions initiated by DOS (**Fig. 5e**). In these cells, DOS-driven TRBV
216 generation commences (**Fig. 4c**). YF-specific signals were not found in those $CD3^{low}$ T_{EMRA} cells that
217 had been pre-exposed to beta catenin or RAG inhibition (Rag1/2 -; **Fig. 5e, f**). Similar results were
218 obtained with longer YF exposure or influenza antigens (30'; **Extended Data Fig. 15a, b**). This
219 revision pathway was essential for subsequent YF-specific stem like TRBV clone generation (**Fig. 5g**).
220 Correspondingly, DOS-driven YF-specific IFN-γ production or TREC generation were disrupted by
221 Rag or beta catenin inhibition (**Fig. 5h-j**). DOS activates Rag mediated TCR revisions in the
222 reprogramed T cells.
223
224 These responses, which were obtained just with DOS prophylaxis and no prior vaccination, are in line
225 with YF specific T cell activities among YF vaccinated individuals[42], similarly to vaccine-free
226 prophylactic treatment of T cells or mice (**Fig. 3** and **Extended Data Fig. 11**). TCR rearrangements
227 were also obtained with common Epstein Bar viral (EBV) antigens and overlapped in part with YF

activation (**Extended Data Fig. 16a**). Reprogramed TCRs with degenerate pockets[43] may protect against a variety of challenges and correlated with generation of new antigen-specific stem like TRBV clones (**Extended Data Fig. 16b**). Rejuvenation confers new functions not previously existent in the younger past of the T cell.

It is possible to rejuvenate and reprogram to T cells, using DOS. We propose a model whereby upon sMAC disruption, β-catenin drives juvenile dependent Rag re-expression activating peripheral TCR rearrangements. Such that, during reprogramming, new antigen specific TCRs can be quickly detected before antigen stimulation occurs. These TCRs possess degenerate pockets that recognize conserved epitopes among different pathogens, providing simultaneous and broad immunological coverage. Thus, unlike vaccination that immunizes against a specific pathogen, reprogramming provides a wider protection against unknown challenges that will be encountered in the future. In this, rejuvenated T cells scan conserved 'danger' signals within the extracellular space via the TCR. These findings are of immediate importance for elderly care and cancer treatment design where immune ageing presents an unmet medical challenge and may be relevant in other cellular systems subjected to rejuvenation.

References

1. Diloreto, R. & Murphy, C. T. The cell biology of aging. *Mol Biol Cell* **26**, 4524-4531 (2015).
2. Ogrodnik, M. Cellular aging beyond cellular senescence: Markers of senescence prior to cell cycle arrest in vitro and in vivo. *Aging Cell* **20** (2021).
3. López-Otín, C., Blasco, M. A., Partridge, L., Serrano, M. & Kroemer, G. Hallmarks of aging: An expanding universe. *Cell* **186**, 243–278 (2023).
4. Soria-Valles, C. & López-Otín, C. iPSCs: On the Road to Reprogramming Aging. *Trends Mol Med* **22**, 713–724 (2016).
5. Takahashi, K. & Yamanaka, S. Induction of Pluripotent Stem Cells from Mouse Embryonic and Adult Fibroblast Cultures by Defined Factors. *Cell* **126**, 663–676 (2006).
6. Lehmann, M. *et al.* Partial Reprogramming As An Emerging Strategy for Safe Induced Cell Generation and Rejuvenation. *Curr Gene Ther* **19**, 248–254 (2019).
7. Jay Sarkar, T. *et al.* Transient non-integrative expression of nuclear reprogramming factors promotes multifaceted amelioration of aging in human cells. *Nat Commun* **11**, 1–12 (2020).
8. Alle, Q., Le Borgne, E., Milhavet, O. & Lemaitre, J.-M. Reprogramming: Emerging Strategies to Rejuvenate Aging Cells and Tissues. *Int J Mol Sci* **22**, 3990 (2021).
9. Xie, H., Ye, M., Feng, R. & Graf, T. *Stepwise Reprogramming of B Cells into Macrophages*. (2004).
10. Vizcardo, R. *et al.* Regeneration of human tumor antigen-specific T cells from iPSCs derived from mature CD8+ T cells. *Cell Stem Cell* **12**, 31–36 (2013).
11. Minagawa, A. *et al.* Enhancing T Cell Receptor Stability in Rejuvenated iPSC-Derived T Cells Improves Their Use in Cancer Immunotherapy. *Cell Stem Cell* **23**, 850-858.e4 (2018).
12. Lanna, A., Henson, S. M., Escors, D. & Akbar, A. N. The kinase p38 activated by the metabolic regulator AMPK and scaffold TAB1 drives the senescence of human T cells. *Nat Immunol* **15**, 965–972 (2014).

13. Lanna, A. *et al.* A sestrin-dependent Erk-Jnk-p38 MAPK activation complex inhibits immunity during aging. *Nat Immunol* **18**, 354–363 (2017).

14. Lanna A *et al.* An intercellular transfer of telomeres rescues T cells from senescence and promotes long-term immunological memory. *Nat Cell Biol* **24**, 1461–1474 (2022).

15. Senior, A. W. *et al.* Improved protein structure prediction using potentials from deep learning. *Nature* **577**, 706-710 (2020).

16. Wolfson, R. L. *et al.* Sestrin2 is a leucine sensor for the mTORC1 pathway. *Science* **351**, 43-48 (2016).

17. Parmigiani, A. *et al.* Sestrins Inhibit mTORC1 Kinase Activation through the GATOR Complex. *Cell Rep* **9**, 1281–1291 (2014).

18. Xiao, B. *et al.* Structural basis for AMP binding to mammalian AMP-activated protein kinase. *Nature* **449**, 496–500 (2007).

19. Sinnett, S. E., Sexton, J. Z. & Brenman, J. E. A High Throughput Assay for Discovery of Small Molecules That Bind AMP-Activated Protein Kinase (AMPK). *Curr Chem Genom Transl Med* **7***,* 30-38 (2013).

20. Sanders, M. J. *et al.* Defining the mechanism of activation of AMP-activated protein kinase by the small molecule A-769662, a member of the thienopyridone family. *J Biol Chem* **282**, 32539-32548 (2007).

21. Müller-Durovic, B. *et al.* Killer Cell Lectin-like Receptor G1 Inhibits NK Cell Function through Activation of Adenosine 5′-Monophosphate–Activated Protein Kinase. *The Journal of Immunology* **197**, 2891–2899 (2016).

22. Pereira, B. I. *et al.* Sestrins induce natural killer function in senescent-like CD8 + T cells. *Nat Immunol* **21**, 684-694 (2020).

23. Zhao, F. *et al.* Paracrine Wnt5a-β-Catenin Signaling Triggers a Metabolic Program that Drives Dendritic Cell Tolerization. *Immunity* **48**, 147-160.e7 (2018).

24. Senni, N. *et al.* β-catenin-activated hepatocellular carcinomas are addicted to fatty acids. *Gut* **68**, 322–334 (2019).

25. Sadot, E., Geiger, B., Oren, M. & Ben-Ze'ev, A. Down-Regulation of β-Catenin by Activated p53. *Mol Cell Biol* **21**, 6768–6781 (2001).

26. Watcharasit, P. *et al.* Direct, activating interaction between glycogen synthase kinase-3 and p53 after DNA damage. *PNAS* **99**, 7951–955 (2002).

27. Gorgoulis, V. *et al.* Cellular Senescence: Defining a Path Forward. *Cell* **179**, 813–827 (2019).

28. Gattinoni, L. *et al.* A human memory T cell subset with stem cell-like properties. *Nat Med* **17**, 1290-1297 (2011).

29. Becker, T. C., Coley, S. M., Wherry, E. J. & Ahmed, R. Bone Marrow Is a Preferred Site for Homeostatic Proliferation of Memory CD8 T Cells. *Journal of Immunology* **174**, 1269–1273 (2005).

30. Akkaya, M., Kwak, K. & Pierce, S. K. B cell memory: building two walls of protection against pathogens. *Nat Rev Immunol* **20**, 229–238 (2020).

31. Takemori, T., Tarlinton, D., Hiepe, F. & Andreas, R. B Cell Memory and Plasma Cell Development. *Molecular Biology of B Cells: Second Edition,* 227–249 (2015).

32. Hale, J. S. & Ahmed, R. Memory T follicular helper CD4 T cells. *Front Immunol* 6, (2015).

33. Gao, X., Wang, H., Chen, Z., Zhou, P. & Yu, D. An optimized method to differentiate mouse follicular helper T cells in vitro. *Cellular and Molecular Immunology* **17,** 779–781 (2020).

34. Yamada, D. H. *et al.* Overcoming CD4 Th1 Cell Fate Restrictions to Sustain Antiviral CD8 T Cells and Control Persistent Virus Infection. *Cell Rep* **16**, 3286–3296 (2016).

35. Li, F. *et al.* Histone deacetylase 1 (HDAC1) negatively regulates thermogenic program in brown adipocytes via coordinated regulation of histone H3 lysine 27 (H3K27) deacetylation and methylation. *Journal of Biological Chemistry* **291**, 4523-4536 (2016).

36. Douek, D. C. *et al.* Changes in thymic function with age and during the treatment of HIV infection. *Nature* **396**, 690-695 (1998).

37. Li, T. T., Han, S., Cubbage, M. & Zheng, B. Continued expression of recombination-activating genes and TCR gene recombination in human peripheral T cells. *Eur J Immunol* 32, (2002).

38. Akondy, R. S. *et al.* Origin and differentiation of human memory CD8 T cells after vaccination. *Nature* **552**, 362-367 (2017).

39. Lantelme, E. *et al.* Cutting Edge: Recombinase-Activating Gene Expression and V(D)J Recombination in CD4 + CD3 low Mature T Lymphocytes . *The Journal of Immunology* **164**, 3455-3459 (2000).

40. Wilson, A., Held, W. & Robson Macdonald, H. Two Waves of Recombinase Gene Expression in Developing Thymocytes. *J Exp Med* **179**, 1355-1360 (1994).

41. Nika, K. *et al.* Constitutively active lck kinase in T cells drives antigen receptor signal transduction. *Immunity* **32**, 766–777 (2010).

42. Gaucher, D. *et al.* Yellow fever vaccine induces integrated multilineage and polyfunctional immune responses. *Journal of Experimental Medicine* **205**, 3119–3131 (2008).

43. Dolton, G. *et al.* Targeting of multiple tumor-associated antigens by individual T cell receptors during successful cancer immunotherapy. *Cell* **23**, 3333-3349 (2023).

Data availability

The data generated or analysed in this study are included in the manuscript, and its Extended data Figures. Next generation TCR sequencing metadata are provided at submission. These data will be available with no restriction for reanalysis and reuse at the point of publication. Source data are available.

Acknowledgments.

We thank A. Sewell for discussions, and D. Escors and L. Fernandez Rubio and Sentcell for technical support. This work was funded by Sentcell ltd. The funder had no role in study design or decision to publish the manuscript. A.L. is a Honorary Professor of the University College London and the Chief Executive Officer of Sentcell ltd.

Authors contributions.

A.L. invented the DOS and further conceived of, designed and directed the study, analysed and interpreted the data, provided fundings and laboratory infrastructures and wrote the manuscript. C.D.A. and F.R. performed experiments and analysed individual data sets. L.C. synthesized sestrin mutants. M.C. performed experiments. M.D.P. analysed human TCR sequencing under guidance of A.L. M.K. provided suggestions. All authors read and approved the final version of the manuscript.

Competing interests.

A.L. is a shareholder to Sentcell ltd and the sole inventor of the DOS pharmaceutics where Sentcell ltd figures as the Applicant (PCT/IT2021/000059). M.K. serves as a scientific advisor to Sentcell ltd. A.L. M.C and F.R. are supported by Sentcell ltd.

Figure. 1 - Discovery of DOS

a, Molecular structure of the lead compound DOS46L (hereafter, DOS). **b**, DOS binding site to Sestrin 2 predicted by AutoDock Vina and AlphaFold algorithms. **c**, Co-Immunoprecipitation of biotinylated DOS46L (DOS; used at 10μM, throughout) followed by recombinant tagged protein detection, as indicated**. d**, Recombinant sMAC activity investigated by liquid scintillation. Cpm, counts per minutes.

e, Half maximal inhibitory concentration (IC50) of DOS against recombinant sestrin-AMPK complexes by *in vitro* kinase assays with SAMS peptides and ADP-glo kinase assessment (**left**); equilibrium dissociation constant (Kd) of sestrin bound biotinylated DOS assessed by ELISA with streptavidin antibodies (**right**). **f**, Quantification of selective DOS penetration in sMAC negative and sMAC positive primary human $CD4^+$ T cells by flow cytometry, 30 minutes after DOS treatment (n = 7 donors). **g**, Individual channels of representative confocal imaging (n = 3 donors) of DOS (green) uptake in human $CD4^+$ T cells. Scale bar, 5 μm. **h**, Co-Immunoprecipitation (IP, hereafter) of biotinylated DOS from human $CD4^+$ T cell extracts after overnight treatment. Presence or absence of sestrin, p38, JNK, ERK (sMAC) or MIOS and WDR59 (GATOR) was confirmed by western blot in the IP. Whole cell lysates (WCL) controls are shown (same extracts; run in parallel). **i**, ERK, JNK and p38 MAPK kinase activity (autophosphorylation) among T_{sen} sestrin 2 immunoprecipitates (sMACs) in the presence or in the absence of DOS for 30 minutes (n = 5 donors). Kinase activity was detected by ELISA assays. **j**, Human T_{sen} were pre-treated with the proteasomal inhibitor MG132 (1μM) for 30 minutes followed by addition of DOS for 2 hours. Controls were not treated with DOS. Total lysates and sestrin 2 immunoprecipitates were then analysed by immunoblotting of ubiquitin and sestrin 2. H3, whole cell lysate control. **k**, Pooled ubiquitination data (n = 5 donors) for experiments as in (**i**). Data are shown as fold change to the untreated control (NO DOS, in the presence of MG132), set as 1. **l**, Time dependent assessment of sestrin expression (1, 2 and 3) by DOS in human T_{sen} (**top**) and AMPK phosphorylation in the same cells assessed by western blotting (**bottom**). Representative of 6 donors. In **e, f, j, k,** one-way Anova with Bonferroni postcorrection for multiple comparisons was performed. **P<0,01; ***P<0,001; ****P<0,0001. Error bars indicate SEM.

Figure. 2 – DOS-driven T cell reprograming

a, Senescence-associated β-galactosidase expression in DOS-treated (DOS-juvenated) or untreated T_{sen}. Cells were purified and cultured for one week in the presence of anti-CD3 (0.5 μg/mL) and rhIL2 (5 ng/mL), then stained to detect β-galactosidase activity. Representative image on the inverted phasecontrast microscope (**left**) and relative quantification (**right**, n = 8 donors). **b**, Population

doublings of human T_{sen} (transduced with irrelevant scramble) and sestrin null $CD4^+$ T_{sen} (transduced by triple lentiviral depletion of sestrins) and cultured as in (**a** ,**left**). Donor-matched $CD27^+$ $CD28^+$ $CD4^+$ T cells (herafter, T_{erl}) were cultured in parallel but activated with anti-CD3 and anti-CD28 (n = 5 donors). Cells were cultured over two weeks with restimulation every 7 days. DOS-driven population doublings (**right**) were calculated as delta between DOS treated and DOS untreated T cells, with or without depletion of sestrins. **c**, DOS-juvenation of human $CD4^+$ T cells. Terminally differentiated effector memory $CD45RA^-$ $CD28^-$ $CD27^-$ $CD4^+$ T cells (hereafter, senescent T_{EM}) were purified and cultured over 20 days, as in (**a**) At day 1 (18 hours), 7, and 21 cell phenotypes were assessed by flow cytometry. Quantifications of rejuvenated stem like ($CD28^+$ $CD45RA^+$ $CCR7^+$ $CD95^+$ $CD62L^+$ $TCF1^+$) among human $CD4^+$ T cells are shown (left; n = 5 donors). Decay of senescent T_{EM} and $CD28^-$ $CD27^-$ $CD45RA^+$ $CD4^+$ T cells (hereafter, senescent T_{EMRA}) undergoing rejuvenation is shown (**right**). **d**, Adoptive transfer of DOS-juvenated T cells, experimental design. Donor T cells were derived from twenty-month-old mice 15 days after Fluad vaccination with or without DOS treatment (0.1 mg/Kg throughout), labeled with Cell Trace Violet (CTV) dye or congenic CD45.1 tracking, then transferred into young naïve CD45.2 recipients (3 months). In parallel, young mice (3 months) were used as young donor control. Recipient animals were rested for 28 days, then analyzed for donor T cell persistence and maintenance of stem phenotype after transfer. **e**, Maintenance of donor DOS-juvenated CD45.1 $CD4^+$ T cells, their aged-matched controls, and that of young donor T cells, 28 days after transfer (day 43) in recipient mouse lymph nodes. Representative flow cytometry plots and poled data (n = 5 mice per group) are shown. **f**, Assessment of stem like transferred T cells (among CD45.1 $CD44^-$ $CD62L^+$ $CD95^+$ $CD4^+$ T cells) and terminally differentiated cells (TE, among CD45.1 $CD44^-$ $CD62L^-$ $CD4^+$ T cells) following adoptive transfer as in (**d)** (n = 5 mice per group). **g**, *IL7R* gene expression and (**h)** CD95 and Sca-1 mean fluorescent intensity (MFI; throughout) in stem cells derived from $CD4^+$ $CD45.1^+$ transferred stem T cells among lymph nodes of recipient CD45.2 mice, 28 days after transfer (n = 5 mice per group). **i**, Representative plots of CD45.1 transferred cells in quiescent state before and after transfer assessed by cycle related intra-nuclear Ki67 staining. Representative of n = 5 mice per group.

j, G1 ($Ki67^+$) to G0 ($Ki67^-$) transition in stem like CD45.1 $CD4^+$ T cells before and after adoptive transfer as indicated (*n* = 5 mice per group). **k**, Assessment of T cell longevity following DOS-juvenation. Cells from lymph nodes were stained using the Annexin-PI Apoptosis detection Kit 28 days after transfer. Representative FACS plot (Left) and quantification of dead $CD45.1^+$ $CD4^+$ transferred T cells (Right). Data are from *n* = 4 mice per group. **l**, DOS-juvenated T cell maintenance, *in vivo* model. In **a, b** (right) two tailed paired T test was used. In **b** (left), **c, e-h, j k** one-way Anova with Bonferroni post-correction for multiple comparisons was used, *p<0,05, **P<0,01; ***P<0,001; ****P<0,0001. Error bars indicate SEM.

Figure. 3 –Reprogramed T cells possess prophylactic functions even without vaccination

a, Adoptive transfer of DOS-juvenated T cells, experimental design. $CD45.1^+$ $CD4^+$ donor T cells were derived from twenty-month-old mice injected with and without DOS (0.1 mg/Kg throughout), then transferred into old naïve CD45.2 recipients (20 months) 72 hours later. In parallel, young (3 month old) naïve CD45.1 mice were used as young $CD4^+$ T cell donor control. Recipient animals were vaccinated, or not, with Fluad the day after, as indicated. Animals were subjected to a lethal H1N1 flu viral infection 8 weeks after transfer, and culled within 15 days of infection. Vaccinated young and old mice were also assessed, to determine background responses. **b**, Survival of mice, Fluad vaccinated, or not, and then challenged with lethal H1N1 infection as in (**a**). Data are from *n* = 5 mice per group. **c**, Fluad-specific IgG production in the same animals subjected to H1N1 infection. Data are from *n* = 5 mice per group. Transfer free vaccinated recipients are shown (**top right; throughout**). **d**, Neutralization properties of Flu-specific IgGs from recipient mice as indicated were assessed upon overnight H1N1 infection of canine kidney cells (MDCK) *in vitro* by ELISA with anti-influenza A NP antibody. Data are from *n* = 5 mice per group. **e**, Viral polymerase acidic protein (PA) assessment in lungs of the same mice upon H1N1 viral infection as in (**a**) by qPCR (*n*=5 mice per group). Data are

462 expressed as fold change to the old, infected control (transferred $CD4^+$ T cells, no DOS), set as 1. **f**,
463 Representative FACS plots and **(g)** pooled data of primary antiviral Th1 responses among T-bet^+ $IFN\gamma^+$
464 CD45.1 donor mouse $CD4^+$ T cells as in (**a**). Data are from *n* = 5 mice per group. **h**, $CD44^-$ $CD62L^+$
465 $CD95^+$ $CD4^+$ T cells (stem-like T cells) in animals subjected or not to $CD4^+$ T cell transfer and then
466 infected in the same experiments as in (**a**); Old naive recipient examples are shown (*n* = 5 mice per
467 group). **i**, The fraction of sestrin expressing donor T cells among adoptively transferred $CD45.1^+$ $CD4^+$
468 T cells from age-matched (20 months) $CD45.2^+$ recipients, six months after transfer as assessed by flow
469 cytometry (*n* = 5 mice per group). In **c-e, g-i,** one-way Anova with Bonferroni post-correction for
470 multiple comparisons was used. In **c** (Top right), **e** (Top right), a two tailed paired T test was used. In **b**
471 Mantel-Cox test was used. *P<0,05; **P<0,01; ***P<0,001; ****P<0,0001. Error bars indicate SEM.
472
473 **Figure. 4 – Reprogramed T cells present *de novo* antigen-specific TCR rearrangements**
474 **a**, Purified human $CD4^+$ T cells and autologous APCs (CD3-depleted PBMCs) were pre-treated or not
475 with DOS or YF peptides (YF) for 4 hours, respectively, then co-cultured for additional 18 hours, in 1:2
476 ratio. The day after, post-synaptic $CD4^+$ T cell genomic DNA was derived from the conjugates and
477 processed for Next generation sequencing (NGS) of the *TCRVB* gene. The table shows inductions of *T*
478 *cell receptor Beta Variant* (TRBV) rearrangements (V-DJ recombination) from a single donor upon YF
479 stimulation of DOS-juvenated $CD4^+$ T cells. For experimental details, please see Methods. One
480 representative donor of 4 is shown. Further genomic clonotypes, **Extended Data Fig.14**. **b**, Antigen
481 pocket rearrangements among TRBV7-1 variant in T cells derived from the same donor as in (**a**).
482 Example of single YF-specific TCR clonotypes (among TRBV7-1) that are only seen in T cells exposed
483 to YF-pulsed APCs, with or without DOS (**bottom**). Note that most antigen pocket rearranging requires
484 presence of DOS, indicating active D-J recombination. **c**, Single cell presence of YF-specific TRBVs
485 among the different T cell subsets of the 4 donors subjected to NGS. The expression levels of each
486 TRBV were evaluated in individual cells by flow cytometry against the unstimulated background. Each
487 dot is a single TRBV in the single cell flow cytometry assessment. No double TRBVs expressing T cells

488 could be detected (**top right**). Results from 4 experiments are shown. **d**, Absence of early YF-specific
489 proliferation (18 hours) of the same stem T cells as shown by CTV tracking. YF-specific TRBV (7.1)
490 clonotypes among the same stem-like T cell clones from 4 different donors, at the same time, is shown
491 (intracellular flow IFN-γ detection; top right). Activation induced markers (AIM) assay of *de novo*
492 TRBV7-1 YF-specific T_{STEM} clonotypes (n = 4 donors, bottom right). Antigen free synapses were
493 subtracted. **e**, IFN-γ release by the indicated TRBV expressing T stem clones after 18-hour YF peptide
494 stimulation and (**f**) antigen-specific proliferation of the same clones, 4 days after culture as assessed by
495 BrdU incorporation. Cell culture conditions as in (**a**). Specificity cell population controls (T_{CM} and T_{EM})
496 are shown. In **c, e** One-way Anova with Bonferroni post-correction for multiple comparisons was used.
497 In **d, f** statistical significance was determined by two tailed unpaired student T test. ***P<0,001;
498 ****P<0,0001. Error bars indicate SEM.
499
500
501 **Figure. 5– DOS restores Rag function via beta catenin during T cell reprograming**
502 **a**, Representative immunoblots (**left**) and quantification (**right**) of Rag protein expression from human
503 $CD4^+$ T cells treated or not with DOS for 4 hours (n = 3 donors). Data are expressed as fold change to
504 the untreated control (no DOS), set as 1. **b**, Rag 2 proteins were immunoprecipitated from the chromatin
505 of human $CD4^+$ T cells treated as in (**a**) then followed by ELISA with anti-Rag 1 and 2 antibodies. Data
506 are expressed as fold change to the untreated control (no DOS), set as 1. **c** and **d**, DOS driven Rag
507 induction in the presence or in the absence of beta-catenin inhibition. Senescent T_{EM} were pre-treated
508 or not with the beta catenin inhibitor ICG-001 (10μM, 30') followed by DOS driven reprograming for
509 4 hours. Rag expression was then investigated by quantitative real time PCR (**c)** and flow cytometry (**d**;
510 n = 4 donors). Note absence of DOS-driven Rag generation in the presence of beta catenin blocking. **e**,
511 YF-specific LCK activation (T394 phosphorylation) among senescent forming T_{EMRA} cultured in the
512 presence or in the absence of beta catenin (ICG-001) or Rag inhibition (Rag- by siRag1/2). Senescent
513 T_{EM} were pre-treated with beta-catenin or Rag inhibition then incubated with DOS for 4 hours, followed

by conjugation with autologous YF pulsed APCs for 5 minutes. Results were stratified by relative CD3 expression. Note that only the forming $CD3^{low}$ T_{EMRA} undergo initial YF specific activation (n = 5 donors). **f**, Representative FACS plot validation (**left**) and quantification (**right**; n = 3 donors) of Rag knockdown in human $CD4^+$ T cells. HEK293T cells were used as negative Rag expression control (**bottom left**). Note that Rag silencing reduces Rag expression to background fluorescence of HEK293 cells naturally lacking Rag proteins, validating known down efficiency. **g**, Rag deficiency abrogates DOS-driven TCR revisions. Human $CD4^+$ T cells were transfected with siCtrl or siRAG1/siRAG2 for 3 days. The T cells were then treated with or without DOS for 4 hours, in the presence or in the absence of beta-catenin blocking (ICG-001) prior to culture with YF-pulsed or antigen-free APCs for 18 hours. The YF specific DOS-juvenated TCRs derived by background subtraction with no YF peptides are shown (n = 4 donors). **h**, Effect of Rag protein silencing on the YF-specific IFN-γ production among the indicated stem like T cell clones or on **(i)**, the YF specific TCR rearrangement, assessed by TREC quantification (n = 4 donors). In **a-d** two tailed paired T test was used. In **e-h** One-way Anova with Bonferroni correction for multiple comparisons. In **f,** F test. *P<0,05; **P<0,01; ***P<0,001; ****P<0,0001. Error bars indicate SEM.

Extended Data Figure 1 – DOS design

a, Schematic representation of DOS compound design strategy. **b**, Workflow of the in vitro screening of DOS compounds. **c**, In vitro screening of DOS compounds. Suppression of AMPK activation upon addition of recombinant sestrin was used as a readout. **d**, Cyclic DOS46L synthesis, the lead compound.

Extended Data Figure 2–DOS-sestrin2 binding, molecular docking

a, 3D representation of sestrin 2 showing the two possible DOS46L binding sites. The interacting amminoacids are shown. Highlighted aminoacids were subjected to inactivating mutagenesis. **b**, Predicted DOS binding site to sestrin 2. Boxes indicate intervention points for mutagenesis. **c**, Confirmation of sMAC disruption sites by DOS was performed by intracellular flow cytometry and showed as fold change to the untreated control (no DOS), set as 1. Alanine scanning mutagenesis was performed in primary human T_{erl} cells (n = 3 donors).

Extended Data Figure 3- Exemplification of DOS discovery

a, Representative FACS plot (**left**) and quantification (**right**) of DOS penetration in human Tsen compared to T_{erl} (n = 8 donors). **b**, DOS treatment does not alter CD4 internalization in purified human $CD4^+$ T cells followed by anti-CD3/CD28 activation (n = 4 donors). **c**, Confocal imaging of sestrin2, DOS46L and the reticulum endoplasmatic KDEL marker. Colocalization in human $CD4^+$ T cells and its individual channels are shown. Representative of n = 3 donors. **d**, sMAC IPs were derived by sestrin 2 pull down from human T_{sen} transduced as indicated. The IPs were treated or not with DOS for 30 minutes in the presence or in the absence of ATP (200 μM) prior to ELISA based in vitro kinase reactions with anti-p-p38. **e**, p38 activity among sestrin 2 IPs (sMACs) derived from human T_{sen} exposed or not to DOS directly in the IP reaction, in the presence or absence of compound C (10 μM). Note that DOS inhibitory action is phenocopied by compound C and no further inhibition of sMAC can be obtained when combining DOS with the AMPK inhibitor (n = 3 donors). In vitro kinase assays detecting p38 MAPK self-phosphorylation reactions upon subtraction of ATP free conditions are shown. **f**, Quantification (n = 5 donors) of sestrin-AMPK binding within sMACs (**wash-in, top**) and their release from the complex (**washout, bottom**). Heatmap of sestrin presence in wash-in and wash-out fractions is shown. sMAC complexes were immunoprecipitated with anti-AMPKa antibodies and incubated with or without DOS for 2 hours, followed by ELISA with anti-sestrin antibodies (sestrin 1, 2 and 3) of both

washin and wash-out fractions in human $CD4^+$ T_{sen}. Data are expressed as fold change to the untreated control, set as 1. **g**, Expression of T_{sen} sMAC components (sestrin 2 and AMPK) with or without DOS (4-hour exposure), in the presence or in the absence of MG132 (10μM) pre-treatment (30 minutes) assessed by immunoblotting. H3, loading control. **h**, (**left**) AMPK activity measured assessing phosphorylation of its downstream target, Acetyl-CoA carboxylase (ACC). Human T_{sen} were treated or not with DOS for 2 or 4 hours and the levels of phosphorylated (p)-ACC and total ACC were evaluated by flow cytometry. AMPK activity was measured as the ratio between pACC and total ACC. Initial AMPK activity (time 0) was set as 1 (100%). Representative plots and pooled data from (*n* = 5 donors) are shown. Compound C treatment was used as control to phenocopy DOS action. (**right**) Confirmation of reduced ACC phosphorylation (Ser79) by immunoblotting, 4 hours after DOS treatment in human $CD4^+$ T_{sen}. Pooled data from (n = 3 donors) are shown. Data are expressed as fold change to the untreated control (no DOS), set as 1. **j**, Representative plot (**left**) and quantification (**right**) of sMAC (sestrin$^+$- p-p38$^+$) presence among human T_{sen}, assessed by flow cytometry with or without DOS treatment (4 hours; *n* = 6 donors). **j**, DOS reversal of irradiated induced senescence, assessed by flow cytometry based sestrin 2 measurements. Human T_{sen} were exposed to X-ray irradiation (8Gy/min, 10min) followed by treatment with DOS for 18 hours. In **b, d, e j,** One-way Anova with Bonferroni postcorrection for multiple comparisons was used. In **a, f, h, i,** two-tailed paired t-test. *P<0,05; **P<0,01; ***P<0,001; ****P<0,0001. Error bars indicate SEM.

Extended Data Figure 4 – DOS-driven AMPK inhibition initiates sMAC dismantling

a, Sestrin 2 and AMPKγ recombinant proteins were incubated at 30 °C. Direct binding was tested by immunoprecipitation of His-tagged AMPK-γ using anti-His tag antibody followed by western blotting. **b**, Investigation of sestrin-driven AMPK activation, assessed via direct ATP loading detection. Recombinant sestrin 2 and AMPK-γ were incubated as in (**a**). ATP was added to each experimental condition and detected after IP washing using the ATP Bioluminescence Assay Kit (*n* = 3 experiments). **c**, AMPK-γ ATP binding in the presence or in the absence of DOS for 5 minutes. The reaction occurred

as in (**b**). In control reactions, AMPK-γ was not incubated with recombinant sestrin 2 but exposed or not to DOS (*n* = 3 experiments). **d**, Recombinant sMAC activity assessed by ADP-Glo kinase Assay with or without the allosteric AMPK activator A769662 (100 μM), in the presence or in the absence of DOS. Note that AMPK allosteric activation is paradoxically increased by co-treatment with DOS, reinforcing the notion that DOS treatment increases ATP loading on AMPK-γ (*n* = 6 experiments). **e**, Fluorescent ATP-binding competition assay. MANT-ATP (10 μM) only fluoresces (448 nm) when bound and was reacted with full-length AMPK (5 μM) or the isolated AMPK-γ subunit (5 μM) in the presence or in the absence of sestrin, in a 1:4 ratio. Note that addition of DOS abolished sestrin-driven ATP unloading, evident as restored MANT-fluorescence in the competition reaction. ATP competition controls for the DOS reaction are shown (*n* = 5 experiments). **f**, Effect of AMPK activity on its binding strength and affinity to sestrin. Non senescent T_{erl} were cultured for 3 days with or without allosteric AMPK activation by A-769662 followed by AMPK-a immunoprecipitation and AMPK-a and sestrin detection. The immunoprecipitates were exposed or not to a denaturating agent (Urea) or further exogenous sestrin 2 (50 ng), to evaluate sestrin binding strength, as indicated. Pharmacological activation of AMPK confirmed by immunoblotting (**left**), and binding disruption data expressed as fold to untreated controls, set as 1 (*n* = 4 donors, **right**). Data are expressed as fold change to the untreated control, set as 1. **g**, Time-course of sestrin-AMPK dissociation upon DOS treatment of T cell sMACs obtained by sestrin 2 immunoprecipitation. T_{sen} cells were treated with DOS as indicated followed by sestrin 2 immunoprecipitation and AMPK-α immunoblotting. IgG, isotype control. **h**, Schematic representation of DOS mechanism of action. DOS impedes sestrin-driven ATP unloading on AMPK-γ leading to AMPK inactivation, loss of sestrin binding affinity, and complex dissociation, culminating with sMAC proteasomal degradation. In **b, f** (**left**), a two-tailed paired t-test was used. In **c-f** (**right**) one-way Anova with Bonferroni postcorrection for multiple comparisons. *P<0,05; **P<0,01; ****P<0,0001. Error bars indicate SEM.

Extended Data Figure 5- DOS action is sMAC specific and occurs via beta-catenin reactivation

a, (**left**) Single cell sMAC sorting, gating strategy. Relative KLRG1$^-$ (sMAC$^-$) vs KLRG1$^+$ (sMAC$^+$) expression was used as single cell sorting strategy. Frequencies and phenotype of sMAC forming T cells is shown. T_{sen}, CD45RA$^{-/+}$ CD28$^-$ CD4$^+$ T cells; T_{CM}, CD45RA$^-$ CD28$^+$ CD4$^+$ T cells. Representative blots of GATOR (mios) and MAPK (phospho-p38) among Sestrin 2 immunoprecipitates in sMAC$^-$ and sMAC$^+$ CD4$^+$ T cell populations, and ELISA based in vitro kinase assays of the precipitated sMACs are shown (**right**). sMAC activity (p38 autophosphorylation) was derived upon ATP based subtractions. Data are from *n* = 4 donors. **b**, Fatty acid oxidation (FAO) levels detected in sMAC$^-$ vs sMAC$^+$ CD4+ human T cells treated or not with DOS for 18 hours, in the presence or in the absence of sestrins. FAO rate was calculated by etomoxir subtraction in Seahorse assessments. Absence of DOS-driven FAO metabolic reprograming among sMAC$^-$ T cells is shown. Sestrin null T cells (shSesn1/23) were derived upon sMAC isolation prior to exposure, or not, to DOS, as a control. Data are from *n* = 4 donors. **c**, p53 protein was immunoprecipitated from sMAC$^-$ vs sMAC$^+$ CD4$^+$ T cells treated with or without DOS for 4 hours followed by ELISA based binding assays with anti-beta catenin antibodies. Data are expressed as fold change to the respective untreated control (no DOS), set as 1 from *n* = 4 donors. **d**, β-catenin binding to T cell DNA 4 hours after DOS driven reprograming in sMAC$^+$ CD4$^+$ T cells was assessed by Chromatin immunoprecipitation (*n* = 4 donors). **e**, Beta-catenin nuclear activation. Luciferase based juvenile report assay of WNT/ beta-catenin signaling promoter in sMAC$^-$ vs sMAC$^+$ CD4+ human T cells treated or not with DOS (4 hours), in the presence or in the absence of sestrins (see Methods). β-catenin mediated transcription was also assessed in the presence or not of p53 activation (nutlin-3, 5μM) and ICG-001 beta-catenin inhibitor (ICG-001 10μM), as a control. Data are from *n* = 4 donors. **f**, Stem like T cell induction among sMAC$^+$ CD4$^+$ T cells treated as indicated in the presence or in the absence of DOS for 18 hours. Data are from n = 4 donors. **g**, Model of DOS driven T cell rejuvenation among sMAC$^+$ CD4$^+$ T cells. In **b-f** One-way Anova with Bonferroni post-correction for multiple comparisons was used, ***P<0,001; ****P<0,0001. Error bars indicate SEM.

642

643 **Extended Data Figure 6 - Effects of DOS-driven reprograming**

644 **a**, T_{sen} were treated with or without DOS for one week in the presence of anti-CD3 and recombinant
645 human (rh)IL2 (*n* = 5 donors). Representative image (**left**) obtained by confocal microscopy and
646 quantification (**right**) of H2AX intensity (MFI, Mean Fluorescence Intensity). Scale bar, 20 μm. **b,**
647 Purified human T_{sen} were activated as in a for 48 hours and then depleted or not of all sestrins using
648 lentiviral particles. Five days after transduction, cells were stained with CTV dye, activated as above
649 then cultured for additional 3 days in the presence or absence of DOS prior to CTV dilution analysis.
650 Representative FACS histograms of *n* = 9 donors. **c**, Human T_{sen} were activated and depleted of sestrins,
651 as above. Five days later, proliferation was assessed by BrdU incorporation for 72 hours in the presence
652 or in absence of DOS (*n* = 5 donors). **d**, Cell-cycle progression (propidium iodide incorporation), and
653 p21 (**e**) (**Top**) and cyclin D1 (**e**) (**Bottom**) protein levels in human T_{sen} cultured as in (**a**) for 3 days (*n*
654 = 4 donors). **f**, Effect of DOS in AMPK null senescent T cells shown by CTV staining (*n* = 3 donors).
655 Human T_{sen} were genetically modified to deplete AMPK, cultured for one month and then stimulated
656 in the presence of CTV for another 3 days. Cells were activated every 7 days (4 round of activations as
657 above) prior to CTV staining to examine proliferation of terminally differentiated cells in culture.
658 Representative FACS histograms (**top**) and quantification of CTV low proliferating cells (**below**). **g**,
659 Senescent markers (p16 and β-Galactosidase) expression in human terminally differentiated T_{EM}
660 directly ex vivo, in $sMAC^+$ or $sMAC^-$ cells. Representative FACS plot (**left**) and quantification (**right**)
661 are shown (*n* = 6 donors). **h**, The effect of DOS on the indicated T cell subsets 10 days after culture (*n*
662 = 8 donors). **i**, The effect of DOS on cytokine production upon senescent TCR ligation was investigated
663 by ELISA among culture supernatants (*n* = 6 donors). **j**, Levels of juvenile related beta-catenin with or
664 without DOS treatment in human stem-like T cells derived from purified T_{sen} cells (*n* = 4 donors). **k**,
665 Representative FACS plots (**left**) and quantification (**right**) of telomere transfer in T_{sen} forming
666 synapses with Ag loaded APCs in the presence or in the absence of DOS. Purified human APCs were

667 labeled with fluorescent telomere probes (Cy3 PNA) and allowed to form synapses with autologous
668 T_{sen} (3:1 ratio; *n* = 5 donors). Data are shown as fold change to the untreated control (no DOS), set as
669 1. **l**, T_{sen} were treated or not with DOS then conjugated with autologous APCs pulsed with
670 Cytomegalovirus (CMV) and Epstein Bar Virus (EBV) antigens (1:50 each) overnight. Post-synaptic
671 T_{sen} and APC genomic DNA was assessed for telomere measurements. Telomere length was calculated
672 from the ΔCT according to the formula suggested by the kit. **m**, Assessment of telomerase activity in
673 T_{sen} 3 days after DOS treatment (*n* = 5 donors). Telomerase activity was detected according to the
674 TeloTAGGG Telomerase PCR ELISA Kit. **n**, Cellular toxicity in human $CD4^+$ T cells in the presence
675 or in the absence of DOS as assessed by Annexin V and PI (*n* = 4 donors). H2O2 treatment, positive
676 death control. In **a,d g-l** , two-tailed paired T test was used. In **c, f,** one-way Anova with Bonferroni
677 correction for multiple comparisons. *P<0,05; **P<0,01; ***P<0,001. Error bars indicate SEM.
678
679 **Extended Data Figure 7 – Central, but not effector, memory T cell phenotypes are enhanced upon**
680 **DOS driven reprograming**
681 **a**, Frequency of central memory (T_{CM}; $CD62L^+$ $CD44^+$) and (**b**) of effector memory (T_{EM}; CD62L-
682 $CD44^+$) among CD45.1 $CD4^+$ T cells recovered from young CD45.2 naïve recipients subjected to
683 adoptive transfer as per **Fig. 3d**. Data are from *n* = 5 mice per group.
684
685 **Extended Data Figure 8 – Phenocopy of CD45.1 T cell longevity in vivo**
686 **a**, Phenocopy of CD45.1 tracking studies. Representative FACS plots, and frequencies of donor CTV
687 $CD4^+$ T cells recovered from young CD45.2 naïve recipients subjected to adoptive transfer as per **Fig.**
688 **4d**, 28 days after adoptive transfer (day 43*; n* = 6 mice per group). Representative pre (**b)** ,and 28-day
689 post (**c**) transfer phenotypes of $CD4^+$ CTV^+ donor T cells from young, old (no DOS) and DOS-juvenated
690 donor mice before adoptive transfer into young recipients. Pre-transfer T cells were assessed 15 days
691 after donor vaccination with Fluad in the presence or absence of DOS as in **Fig. 3d**. CD95 FMO controls

692 are shown. **d**, Frequency of stem like ($CD44^-$ $CD62L^+$ $CD95^+$) and terminally differentiated (TE;
693 $CD62L^-$ $CD44^-$) $CD4^+$ T lymphocytes 28 days after transfer (day 43) in the CTV adoptive transfer
694 model. Data are from *(n* = 5 mice per group). **e**, Sca1 and CD95 protein levels in CTV^+ $CD4^+$ stem T
695 cells in the same recipient mice, 28 days after cell transfer (*n* = 5 mice per group). MFI values are
696 shown. **f**, IL7R gene expression among sorted CTV^+ $CD4^+$ T cells purified form lymph nodes of
697 recipient mice as indicated (*n* = 5 mice per group). **g**, FACS histograms of the cell cycle marker Ki-67
698 among CTV^+ $CD4^+$ donor T cells before and after adoptive transfer. An example of identical Ki67
699 staining before and after transfer is shown. In **a, d-f**, One-way Anova with Bonferroni correction for
700 multiple comparison. ***P<0,001; ****P<0,0001. Error bars indicate SEM.
701
702 **Extended Data Figure 9 - $CD4^+$ T cell reliance of DOS**
703 **a**, Experimental design. Twenty-month-old CD45.1 mice were injected or not with DOS and sacrificed
704 72 hours later. Purified $CD4^+$ T cells or all other $CD4^-$ immune cells were derived from total donor
705 splenocytes. The cells were then transferred into age-matched, old CD45.2 recipient mice vaccinated
706 with Fluad after transfer. Young $CD4^+$ T cells from naïve animals were transferred in parallel and
707 compared against DOS_{juv} $CD4^+$ T cells. Fifteen days later, Fluad-specific serum IgG1s and lymphoid B
708 cell phenotypes were assessed. Young (3 months), old and DOS treated (transfer) mice were also
709 vaccinated and shown throughout as a control. **b**, Fluad-specific induction of memory $CD19^+$ IgG^+ B
710 cells in vaccinated old recipients subjected to adoptive transfer of DOS-juvenated $CD4^+$ T cells (DOS_{juv}
711 T cells), their DOS $CD4^+$ T cell depleted splenocytes (DOS cells ($-CD4^+$)), their aged matched $CD4^+$ T
712 cells from old donor animals not exposed to the DOS ($CD4^+$ T cells (No DOS)) or young $CD4^+$ T cell
713 transfer from naïve donors. Animals with and without vaccination but not subjected to adoptive transfer
714 are shown, with or without DOS treatment (transfer free). Memory cells were pre-gated on CD38, as
715 shown. Representative plots (**left**) and pooled data from (*n* = 5 mice per group) are shown. Lymph node
716 cells were studied. **c**, Circulating Fluad specific IgG1 in the recipient immunized animals were assessed
717 by ELISA 15 days after vaccination. Data are from *n* = 8 mice (transfer-free; young), *n* = 6 mice

(transfer-free; old), *n* = 7 mice (transfer-free; DOS), *n* = 10 mice ($CD4^+$ T cells (NO DOS)), *n* = 13 mice (DOS cells ($-CD4^+$)), or *n* = 15 mice (DOS_{juv} T cells), or *n* = 12 mice (young $CD4^+$ T cells) are shown. Absolute titration data, top left. **d**, Human PBMCs from old donors (age 65-80) were depleted or not of $CD4^+$ T cells. Cells were then cultured for 14 days with Fluad vaccines in the presence or in the absence of DOS. ELISA assay was performed as above described. Data from *n* = 6 donors (young), *n* = 5 donors (old No DOS), *n* = 5 donors (old DOS $CD4^-$), *n* = 6 donors (old DOS) are shown. In **b-d**, one-way Anova with Bonferroni post-correction for multiple comparisons was used, **P<0,01; ***P<0,001; ****P<0,0001. Error bars indicate SEM.

Extended Data Figure 10- DOS_{juv} $CD4^+$ T cells are essential for Ag-specific B cell generation

a, b Representative plots (**left**) and quantification (**right**; *n* = 5 mice per group) of Fluadspecific induction of (**a**) $CD19^+$ $CD38^-$ $GL7^+$ germinal center (GB) B cells and (B) $CD19^{-/low}$, $CD45R^{-/low}$ (B220) $CD138^+$ plasma cells in vaccinated old recipients subjected to adoptive transfer. Recipient animals were injected with DOS-juvenated $CD4^+$ T cells (DOS_{juv} T cells), their DOS $CD4^+$ T cell depleted splenocytes (DOS cells ($-CD4^+$)), their aged matched $CD4^+$ T cells from old donor animals not exposed to the DOS ($CD4^+$ T cells (No DOS)) or young $CD4^+$ T cell transfer from naïve animals. Recipient animals were vaccinated with Fluad one day after adoptive transfer. Young, old and DOS treated animals vaccinated without adoptive transfer are also shown, as per **Extended Data Fig.8**. Lymph node cells were studied two weeks after vaccination (day 15). **c**, $CXCR5^+$ $PD1^+$ Tfh detection among $CD45.1^+$ $CD4^+$ T cells subjected to adoptive transfer in old CD45.2 recipients and analyzed 15 days after recipient Fluad vaccination. Representative FACS plots (**left**) and pooled data (**right**) from (*n* = 5 mice per group) are shown. A background example of vaccinated old transfer-free animals is shown. **d**, Experimental design. $CD4^+$ T cells were purified from total splenocytes of unvaccinated old mice (20 months) then transduced with sh-Scramble or triple shSestrins (sh-sestrin1, sh-sestrin2, shsestrin3). After 96 hours, transduced $CD4^+$ T cells were cocultured with autologous APCs in the presence or in the absence of Fluad (1:100 of the human dose). After additional 10 days, plasma cells were characterized. Antigen

744 specific plasma cells are derived by subtraction of stimulated samples against unstimulated background
745 controls, with or without DOS. **e**, Antigen-specific plasma cell generation in immune cultures as in (**d).**
746 Note that sestrins silencing in old $CD4^+$ T cells phenocopies DOS action. As such, no further induction
747 of antigen-specific plasma cells can be obtained when DOS is added to cultures with sestrin deficient
748 $CD4^+$ T cells (n = 5 mice per group). Young B cell cultures were used as control. In **a-c, e** one-way
749 Anova with Bonferroni post-correction for multiple comparisons. *P<0,05; ***P<0,001; ***P<0,0001.
750 Error bars indicate SEM.
751
752 **Extended Data Figure 11 – Phenocopy of T cell reprograming by systemic DOS administration**
753 **a**, Experimental design. Eighteen-month-old mice were vaccinated with Fluad and injected or not with
754 DOS. After 18, 36 days and 8 weeks mice were bled to detect Fluad specific IgG production. Six months
755 later, mice were infected with lethal H1N1 flu virus and then monitored for survival. Mice were culled
756 within 15 days. Young mice (3 months) were used as control. **b**, Antigen-specific IgG production in
757 young, old and DOS-juvenated mice upon Fluad immunization. For 18 days post-immunization, data
758 are from n = 7 mice (young), n = 6 mice (old), n = 9 mice (DOS). For day 36, data are from n = 7 mice
759 (young), n = 5 mice (old), n = 9 mice (DOS). For week 8, data are from n = 7 mice (young), n = 10 mice
760 (old), n = 10 mice (DOS). Mice were bled at the indicated time points and circulating serum vaccine-
761 specific IgG levels were detected by ELISA. **c**, Survival of mice, vaccinated and challenged with a
762 lethal H1N1 infection, 6 months later as in (**a**), at 24 months of age. Data are from n = 7 mice per group
763 (young and old) and n = 8 mice (DOS). **d**, Fluad-specific IgG production in the same animals 15 days
764 after H1N1 viral infection. Data are from n = 7 mice (young), n = 6 mice (old) or n = 10 mice per group
765 (DOS). **e**, Neutralization properties of Flu-specific IgGs were assessed upon overnight H1N1 infection
766 of canine kidney cells (MDCK) in vitro by ELISA with anti-influenza A NP antibody. Results with heat
767 inactivated sera from DOS-juvenated mice, their aged, matched controls without DOS, and young
768 animals are shown. Data are from n = 7 mice (young), n = 6 mice (old) or n = 10 mice per group (DOS).
769 **f**, Terminal assessment of $CD44^-$ $CD62L^+$ $CD95^+$ $CD4^+$ T cells (stem-like T cells) 231 days after DOS

770 treatment, in splenocytes from old animals infected as in (**a**). Aged matched and young infected animals
771 not exposed to the DOS are shown (*n* = 6 mice per group). **g**, Experimental design. Eighteen-month-old
772 mice were injected with or without DOS, in the absence of Fluad vaccination. Mice were then infected
773 with H1N1 virus after 48 hours, or, in parallel, after 8 weeks to assess survival and anti-viral immune
774 responses to either early or late infection, respectively. Young mice (3 months) were used as control. **h**,
775 Survival of animals as in (**g**) was assessed (*n* = 10 mice per group). **i**, Detection of Flu-specific IgGs
776 among the same animals infected in the early and long-term protocol. ELISA plates were coated with
777 H1N1 viral extracts, rather than Fluad, to detect viral specific antibodies. Data are from n = 10 mice
778 (young), n = 7 mice (old), *n* = 8 mice (DOS early infection (inf. throughout)) or *n* = 9 mice (DOS late
779 inf.). **j**, Neutralization properties of Flu-specific IgGs from DOS-juvenated mice serum, age-matched
780 infected animals not exposed to the DOS or young, infected animal serum (as in (**g**)), with no prior
781 immunization, as in (**i**). **k**, Images of autoptic lungs from representative old mice treated with or without
782 DOS then infected with H1N1 8 weeks later. Young, infected lungs are shown. Organs were collected
783 6 days after infection. Note absence of lung necrosis with the DOS only regimen (no vaccination). **l**,
784 Viral polymerase acidic protein (PA) assessment in lungs of young, old or DOS juvenated mice upon
785 H1N1 viral infection (as in (**a**); *n*=4 mice per group). Data are expressed as fold change to the old,
786 infected control (no DOS), set as 1. **m**, Assessment of stemlike T cells upon DOS juvenation after H1N1
787 viral infection in the early and long-term protocol. Representative FACS plots (**left**) and quantification
788 (**right**, *n*=8 mice per group). **n,** Primary antiviral Th1 responses among T-bet$^+$ IFNγ^+ CD4$^+$ T cell of
789 young, old or DOS juvenated mice to H1N1, 3 days after infection (*n* = 5 mice). In **b, d-f, I, j, m,**
790 **(right) ,n** oneway Anova with Bonferroni post-correction for multiple comparisons was used. In **c, h**
791 Mantel-Cox test was used. *P<0,05; **P<0,01; ***P<0,001; ****P<0,0001. Error bars indicate SEM.
792
793 **Extended Data Figure 12– Single DOS administration induces long-term sestrin inhibition in vivo**
794 **a**, Time course of sestrin 2 expression (MFI) in vivo between DOS treated and vehicle injected mice.
795 Old mice (*n* = 5 mice per group) were subcutaneously injected with DOS, then bled for CD4$^+$ T cell

796 sestrin 2 assessment at the indicated time points. Young $CD4^+$ T cells are shown. MFI, mean
797 fluorescence intensity. **b**, Immunoblot analysis of sestrin 2 inhibition (**left**) and quantification (**right**)
798 among circulating mouse $CD4^+$ T cells treated or not with DOS and assessed 72 hours later.
799 Representative of $n = 4$ animals per group. Data are expressed as fold change to the untreated control
800 (no DOS), set as 1. **c**, Sestrin 2 levels in splenocytes of young, old and DOS-juvenated mice in the
801 presence of Fluad vaccines (10 days post treatment). Quantification of sestrin 2 expression levels
802 assessed by qPCR. Data are from $n = 4$ mice (young), $n = 4$ mice (old) or $n = 6$ mice (DOS). **d**, Sestrin
803 protein levels six months after systemic DOS treatment. Representative FACS plots and pooled data
804 from ($n = 5$ mice per group) are shown. **e**, Investigation of sestrin acetylation (H3K27ac in the sestrin
805 2 locus) among splenocytes of old infected animals (20 months) treated or not with DOS and assessed
806 10 weeks later ($n = 6$ mice per group). Young (3 months) infected animals served as control. The Sestrin
807 2 gene locus was analyzed by qPCR after chromatin immunoprecipitation (ChIP) with anti-H3K27ac
808 antibody. **f**, Evaluation of HDAC1 activity. $CD4^+$ T cell HDAC1 was immunoprecipitated from
809 lymphoid organs of mice as in e and incubated for 30 minutes (30 °C) with exogenous T cell DNA
810 purified from old mice not exposed to DOS ($n = 5$ mice per group). HDAC1 activity (direct deacetylase)
811 was assessed by ELISA assay by detecting H3K27 acetylation levels in target DNA. In **a,c-f,** one-way
812 Anova with Bonferroni post-correction for multiple comparisons. *P<0,05;**P<0,01;
813 ***P<0,001****P<0,0001. Error bars indicate SEM.
814
815 **Extended Data Figure 13 – Reprogramed T cells present functional TCR revisions**
816 **a**, TCR rearrangements measured as TREC quantification from $CD4^+$ T cell genomic DNA purified
817 from lymph-nodes of old H1N1 infected mice (20 months) treated or not with DOS (0.1mg/kg). TREC
818 levels were assessed by qPCR. Young, infected mice (3 months) served as control. **b**, Quantification
819 **(left)** of TCRVβ variant usage in $CD4^+$ T cells purified from lymphnodes of young, old and DOS-
820 juvenated mice (as above) assessed by flow-cytometry, 2 weeks after infection. Viral specific TCR
821 inductions are shown (**right**). **c**, TREC quantification in DOS_{juv} $CD45.1^+$ $CD4^+$ or other transferred T

cells (as indicated) derived from lymph-nodes of old CD45.2 mice subjected to lethal H1N1 infection in the absence of vaccination and assessed 2 weeks later. **d**, Negative selection among DOS_{juv} $CD45.1^+$ $CD4^+$ T cells 28 days after transfer. **e**, Time course of TCR rearrangements assessed by TREC quantification in human $CD4^+$ T cells treated with DOS. $CD4^+$ T cells were activated with anti-CD3/CD28 and rhIL2 and assessed at indicated time points. Data are from $n = 12$ donors (18 hours; 3 days), or $n = 9$ donors (7 days). Absolute raw data are shown. **f**, Generation of YF-specificity upon DOS treatment. $CD4^+$ T cells were pre-treated with or without DOS for 4 hours then conjugated with autologous APCs preloaded with different YF-vaccine dilutions, as indicated. IFN-γ production was investigated in the T_{STEM} compartment by flow cytometry 18 hours later ($n = 6$ donors). Note absence of YF responses in T cells not exposed to DOS, regardless of the antigen dosing. Specificity T cell population controls (T_{CM} and T_{EM}) did not produce any YF response (**top right**). **g**, T_{STEM} were derived from YF-vaccine primed APC-T cell conjugates 18 hours after culture, rested for additional 5 days then re-challenged with autologous YF-vaccine loaded APCs for 18 hours. IFN-γ release was quantified by ELISA in the culture supernatants ($n = 4$ donors). Specificity T cell population controls (T_{CM} and T_{EM}) are shown. **h**, Example of human T_{STEM} gating strategy for YF peptide stimulation with or without DOS (note TCF1 staining confirming 100% stem like T cell origin). Individual gating and positive (PMA-ionomycin induced) IFN-γ induction controls are shown. Yellow shadows, YF specific interval response. **i**, (**top**) quantification of IFN-γ production among the same stem-like human T cells as in (**h**). Autologous APCs and T cells were pre-treated with peptides or DOS respectively for 4 hours prior to co-culture. Yellow fever specific IFN-γ producing stem cells are derived by subtraction against unstimulated backgrounds, with or without DOS (**i**, **bottom**). No response could be detected using a negative peptide control (actin; 2μg/mL), confirming induction of YF specific responses. Absolute IFN-γ producing T_{STEM} counts are shown ($n = 5$ donors). **j**, Generation of YF-specific responses, transgenic T cell controls. OT-II T cells were conjugated with congenic YF pulsed APCs for 18 hours followed by stem-like $CD4^+$ T cell sorting. Five days later, purified stem-like T cells were restimulated as above and YF-specific IFN-γ release was quantified among culture supernatants by ELISA (**top**). In control

experiments, OT-II T cells were derived from animals that had been immunized with ovalbumin, 15 days after vaccination. The recall response to OVA was used as a control to quantify antigen-specific IFN-γ release against the transgenic T cell antigen (OVA; bottom). OVA, ovalbumin. *n* = 5 mice per group throughout. In **a-c,i-j**, One-way Anova with Bonferroni correction for multiple comparisons. In **e** F test. In **f-g** two tailed paired T test was used. *P<0,05; **P<0,01; ***P<0,001; ****P<0,0001. Error bars indicate SEM.

Extended Data Figure 14 – DOS-driven YF-specific TCR clonotypes

a, Yellow Fever (YF) induced TCRs table list referred to Donor A in Fig. 5. **b**, Single TCR clonotypes among different conditions in the Donor D.

Extended Data Figure 15 – DOS-driven Ag-specific TCR activation at a later time point

a, YF-specific LCK activation among senescent T cells cultured in the presence or in the absence of β–catenin or Rag inhibition as in **Fig. 6e**. TCR sensitivity (p-Lck) was assessed 30 minutes upon YF stimulation. Results were stratified by relative CD3 expression. Note that only $CD3_{low}$ T cells undergo antigen specific activation (*n* = 5 donors). **b**, Flu-specific activation among senescent T cells cultured as in (**a**). Note that DOS has only effects on the $CD3l_{ow}$ T cells undergoing rejuvenation (*n* = 5 donors). One-way Anova with Bonferroni correction for multiple comparisons was used. ****P<0,0001. Error bars indicate SEM.

Extended Data Figure 16 - DOS generates unique antigen specific TRBV clonotypes

a, Additional examples of other unique human VDJ clonotypes (among TRBV7-1) with de novo YF specific antigen pockets originating upon synapse interactions with APCs, in the presence or in the absence of DOS (**left**). Examples of unique EBV specific clonotypes with new antigen pockets as per YF in the same donors are shown (**Right**). **b**, Correlation of YF-specific TRBV7.1 expressing $CD3^+$, $CD4^+$, $CD28^+$, $CD45RA^+$, $CD95^+$, $CD62L^+$ stem T cells and unique YF-specific de novo clonotypes in

the same TCRV, with or without DOS (**left**). A ratio response for productive (IFN-γ^+) TCRBV and the unique clonotypes formed is proposed ($n = 4$ experiments; right). In **b,** two tailed paired T test was used. *P<0,05. Error bars indicate SEM.

Materials and Methods

Human and mouse studies

All human specimens were obtained from de-anonymized volunteers unless otherwise specified with the approval of Tuscany Life Sciences Ethical Committee and voluntary informed consent in accordance with the Declaration of Helsinki in all cases. No compensation was offered. For mouse studies, we received approval from the Italian Ministry of Health. Mouse husbandry was controlled by standard circadian rhythms (12 hours of dark and 12 hours of light; fixed temperature 25°C, humidity between 40-60%). For ageing studies, old donors were 65-80 years old.

DOS synthesis and formulation

The synthesis of c-DOS46L consisted of four stages. In stage 1 the naked linear peptide, CDOS1, was generated. Specifically, the first amino acid (Fmoc-Val-OH) was loaded on the 2-CTC resin and then the Fmoc was deprotected using Piperidine in DMF. The remaining 4 amino acids were coupled one by one in predetermined sequence using HOBt and DIC. Followed deprotection of Fmoc group using Piperidine in DMF, after each amino acid protection to avail for next amino acid coupling to elongate the chain. In the end of this step the crude linear peptide was obtained with a charge of 2%TFA /DCM to knock off the resin.

Stage 2 was aimed to obtain the crude cyclic peptide, CDOS2. This was obtained by cyclization of the linear peptide by using EDC. HCl/HOBt.H_2O/ DIPEA in DMF as a solvent.

In stage 3 the CDOS2 was charged on the Reverse phase column to yield the pure cyclic peptide, CDOS3. In the end, in stage 4, the column pooled fractions were distilled to minimum desired level and

then filtered, the material was then dried at 55"5°C under vacuum to obtain the targeted pure cyclic peptide, CDOS4. CDOS4 means the C-DOS46L used in all the paper.

Other DOS compounds were synthetized using the same procedure, NH_2COOH cyclisation and FMOC deprotection.

The DOS used in the paper was resuspended in 100% of DMSO (Sigma); subsequential dilution were done in PBS. For pharmacokinetic (PK) studies, DOS was instead resuspended in a solution of 80% PG (propylene glycol) and 20% PEG (Polyethylenglycolum 400). In all the experiments, DOS refers to 10 µM of cyclic DOS46L unless otherwise specified.

DOS peptide library in vitro screening by inhibition of AMPK1

The screening was performed using the kit ADP-Glo kinase Assay (V6930; Promega). Specifically, 250 ng of the recombinant AMPK1 (P47-110GH-10; Signal Chem) were pre-incubated with 10 µM of DOS peptide, before the addition of the pre-incubated complex containing 1 µg of sestrin1 (GWB5DFF50; Genway) or sestrin2 (GWB-66FAFC; Genway), ATP (200 µM; V915B; Promega), AMP (200 µM; V506B; Promega) and SAMsite (0,2 µg/µl; S07-58-1MG; Signal Chem). In addition, in some experiments testing the effect of DOS on the AMPK activity we added to the reaction the AMPactivated protein kinase activator A-769662 (100 µM; ab120335), as indicated.

AMPK activity was then detected by adding 40 µl of kinase detection reagent according to manufacturing protocol. Luminescence was acquired at the Varioskan reader (ThermoFisher).

Background AMPK activity without sestrin was subtracted.

Cell isolation and culture

Peripheral blood mononuclear cells (PBMCs) were isolated by Ficoll (17-1440-03; GE Healthcare) density gradient centrifugation from blood of healthy volunteers.

Primary human $CD4^+$ T cells were isolated using CD4 MicroBeads (130-045-101; Miltenyi); primary human senescent $CD4^+$ $CD27^-$ $CD28^-$ T cells (thereafter T_{sen}) were isolated using $CD4^+$ T Cell Isolation

Kit (130-096-533; Miltenyi) followed by depletion of $CD27^+$ and $CD28^+$ T cells using CD27 antibody. $CD3^-$ cells (thereafter APCs) were isolated by depleting $CD3^+$ cells using human CD3 MicroBeads (130-050101; Miltenyi). The $CD27^+$ expressing population of human $CD4^+$ T cells that co-expresses also CD28 (13,14) was used as early differentiated (non-senescent) T cell (T_{erl}) control. For isolation of mouse T cells, CD4 (L3T4) MicroBeads (130-117-043; Miltenyi) were used. All the isolations were conducted following the manufacturer's protocols.

T_{erl} cells were cultured in RPMI1640 (R2405; Sigma-Aldrich) supplemented with 10% FBS (F9665; Sigma-Aldrich) and 1% Pen-Strep (DE17-602E; Lonza). Dynabeads Human T-Activator CD3/CD28 (11161D; Gibco; 1:100) or plate bound with anti-CD3 and anti-CD28 antibodies (0.5µg/ml each; Invitrogen and Miltenyi) were used to activate these T cells as indicated by the manufacturer protocol. For primary human highly differentiated senescent T_{sen} cell cultures, plate bound CD3 and recombinant human IL2 (5ng/mL) were used instead as previously described[1,2]. For primary cultures, all T cells were incubated in RPMI 1640 media (R8758-500ml; Sigma-Aldrich) supplemented with 10% FBS (fetal bovine) in an incubator (37 °C and 5% of CO_2).

Single cell sMAC isolation

Following human PBMCs isolation, $KLRG1^+$ and $KLRG1^-$ (thereafter $sMAC^+$ and $sMAC^-$ respectively) were purified by fluorescence-activated single cell with > % 99 purity, using BD FACS Melody sorter equipped with three lasers, nine colors and eleven parameters. To reduce stress-induced MAPK activation, background the system is also equipped with sheath filter nozzle with 100 nm pore size that allowed to apply a gentle pressure of 40 psi to sheath fluids, minimizing further stress-induced signals to the cells.

Western blotting protocol

Analysed samples were lysed with RIPA buffer plus phosphatase and protease inhibitors. Protein lysates were quantified by Lowry protocol and then denatured with Lemmli buffer + β- Mercaptoethanol. 7.5

μg of proteins were separated on polyacrylamide gel and then transferred on nitrocellulose membrane by the Trans-Blot dry system (Biorad). Membranes were blocked on milk (5%) or BSA (5%) depending on if the protein to detect were phosphorylated or not.

A comprehensive list of primary and secondary antibodies used for western blotting is reported in table S1. Primary antibodies were used 1:1000 dilution unless otherwise specified. For secondary antibodies 1:5000 dilution was used.

Immunophenotypic analysis

All extracellular stainings were performed resuspending cells in the necessary antibody mix (1:100) in PBS with 0.5% BSA and 2mM EDTA for 30 minutes at 4°C in the dark. If intracellular staining was necessary, cells were then fixed with BD Cytofix Fixation Buffer (554655; BD Bioscience) for 15 minutes at 37°C and permeabilized with BD Phosflow Perm Buffer III (558050; BD Bioscience) for 30 minutes at -20°C. Cells were then stained with either primary conjugated antibody (30 minutes at 4°C) or unconjugated primary antibody (1 hour at 4°C in the dark) followed by a secondary conjugated antibody diluted 1: 500 (30 minutes at 4°C in the dark). Cells were analysed on a CytoFLEX flow cytometer (Beckman Coulter). Dead cells were excluded. A comprehensive list of antibodies used for flow cytometry is reported in Table 2.

Luciferase assay

For the detection of Wnt/ Beta-Catenin activity, purified $sMAC^-$ *vs* $sMAC^+$ $CD4^+$ T cells were plated at a density of 100000 cells per well, in a white opaque 96-well plate. Cells were transduced with 10 ml of TCF/LEF Luciferase Reporter Lentivirus (#79787; BPS Bioscience) and 5 mg/ml of Polybrene (Lenti-Fuse Polybrene Viral Transduction Enhancer #78939; BPS Bioscience) and incubated at 37 °C for 72 hours. After 3 days, culture medium was replaced and cells were pre-treated (30') or not with p53 activator Nutlin-3 (5 mM, #N6287; Sigma-Aldrich), or the beta catenin inhibitor ICG-001 (10 mM, #5047120001, Sigma-Aldrich), with or without DOS for additional 4 hours, as indicated. In some

977 experiments, the sMAC$^+$ T cells were subjected to shRNA sestrin depletion as a control. After 4 hours,
978 100 ml per well of One-Step Luciferase Reagent (#60690; BPS Bioscience) were added and incubated
979 at room temperature for 20 minutes. Luminescence was measured using LUX Multimode Microplate
980 reader (ThermoFisher). A cell-free control was used to subtract the background luminescence.
981
982 **Confocal imaging**
983 To investigate intracellular localization of DOS, 1*10^6 of purified CD4$^+$ T cells were activated with
984 anti-CD3/CD28 and treated with 10 μM of DOS-FITC for 4 hours. Cells were then collected and plated
985 in coverslips pre-treated with poly-lysine and fixed with formaldehyde 4%. Cells were then stained with
986 the primary antibody anti-CD3 (1:100; 14-0037-82; eBioscience) and with a secondary anti-mouse
987 antibody conjugated with AF-647 (1:250; Invitrogen).
988 To check the co-localization of DOS with the ER, 1*10^6 of purified human CD4$^+$ T cells were treated
989 with DOS-FITC for 4 hours and then stained with primary antibody anti-KDEL (1:100; ab12223;
990 Abcam) and anti-sestrin 2 (1:100; Gentex). Secondary antibodies used were anti-mouse
991 conjugatedAF647 (1:250; Invitrogen) or anti-rabbit conjugated-AF594 (1:250; Invitrogen).
992 To evaluate the impact of DOS on DNA degradation, T_{sen} were purified as above described and then
993 treated or not for one week with DOS. 5*10^5 cells were then plated in a poly-lysine pre-coated coverslip
994 and surface-stained with the anti-CD4 antibody APC-Vio 770 (1:100; Miltenyi). Cells were then fixed
995 with 4% formaldehyde and permeabilized with 0,25% Triton (T8787; Sigma). Cells were firstly
996 intracellularly stained with primary rabbit anti-human H2AX antibody (1:100; 2595S; Cell Signaling);
997 and then with secondary anti-rabbit conjugated-AF488 antibody (1:250; ThermoFisher). For all
998 imaging experiments, sections were mounted in a glass slide with ProLong gold antifade mountant with
999 DAPI (P36931; Invitrogen) and fluorescence images were acquired on an Axio Observer confocal
1000 microscope (Zeiss).
1001
1002

Analysis of DOS incorporation

PBMCs were treated with 10 µM DOS-FITC conjugate for 30 minutes, washed, fixed and then immediately analysed by flow cytometry. Surface staining to CD4, CD8, CD27 and CD28, CD62L, KLRG1 receptors and sestrin2 and p-p38 (sMAC) intracellular staining allowed investigation of incorporation of DOS in the different T cell subsets.

Inhibitor concentration 50 (IC50)

To study the IC50 of DOS toward sestrin driven AMPK activity, a mix containing DOS peptides (in 5-fold dilutions between 50 µM and 1 pM), 5 ng/µl recombinant sestrin 2, 50 µM DTT, 0.2 µg/µl SAMsite, 200 µM ATP and 200 µM AMP and 5 ng/µl recombinant AMPK was diluted in kinase buffer as per initial *in vitro* DOS screening. Reaction volume was 25µl coating a 374 well plates.

The mix was incubated for 1 hour at room temperature and the inhibition of sestrin driven AMPK activity was measured following the ADP-Glo kinase Assay kit. Data were analyzed following the manufacturing information of the kit; specifically, the IC50 value was extrapolate via Sigmoidal, 4PL, X is log(concentration) non-linear regression analysis model- GraphPad Prism software.

Sestrin-driven AMPK activity assay by radiolabeled ATP

Commercial recombinant AMPK protein (P47-110GH-10; Signal Chem) was used in combination with recombinant sestrin 2 protein (GWB-66FAFC; Genway). The reaction was performed with 200µM AMP, 200µM ATP (0.5 µCi 32P-ATP per reaction) 50µM SAMS, 250 ng AMPK and 1mg of Sestrin2 in the presence of a kinase buffer (40 mM EDTA, 5mM MgCl2, 0,025% BSA, 0,8mM DTT). After 30 minutes of incubation at 30°C, the reaction was stopped by adding 80µl of H3PO4 1%. Reaction mixture was then transferred to 96 well Multiscreen plate (MAPHNOB50; Millipore) followed by detection in a TopCount® NXTTM.

KD titration curve

Recombinant Sestrin2 was diluted in TBS, pH 7.4, 2 mM $MgCl_2$ at a final concentration of 5 µg/ml and used to coat 96 well plates overnight at 4°C. Coated plates were washed twice with TBS to remove residual soluble proteins and blocked in TBS 1% BSA solution for 1hour at room temperature. A serial DOS-biotin dilutions were prepared in duplicates in TBS 1% BSA and incubated in Sestrin2 coated plates for 90 minutes at room temperature followed by washing steps to remove unbound DOS. The binding between DOS-biotin and Sestrin2 was fixed by using 2,5% of Glutaraldehyde in HBS (50 mM HEPES/NaOH, pH 7,4; 150 mM NaCl). Sestrin2-bound DOS was quantified by ELISA. Primary antibody (streptavidin-HRP 1:2000) was incubated in 50 µl of TBS 1% BSA 90 minutes at room temperature. To detect antibody, 50 µl of TMB substrate (N301; ThermoFisher) was added to each well, incubated for 30 minutes, and reaction was stopped with stop solution (N600; ThermoFisher). The optical density (OD450) was measured by an ELISA on a microplate reader (AMR-100, Biolab). KD was calculated in GraphPad Prism by performing a "Non-linear regression statistical analysis" with the following equation[3]:

$$Y= (S_{max}-S_{min})*((X+R+K)-sqrt((X+R+K)^2-4*R*X))/(2*R)+S_{min}+B*X$$

Where:

Y being the signal value S

X being the concentration of added DOS

R being the concentration of immobilized protein

K being the dissociation constant

B being the background slope

***In vitro* pull down with biotinylated-DOS**

0.1µg/µl of recombinant tagged proteins (sestrin1-FLAG-tagged; sestrin2-FLAG-tagged; AMPK1His-tagged) were incubated with 10 µM of DOS-biotin overnight at 4°C. Streptavidin-agarose beads (20353; Thermo Scientific) were washed with PD buffer (20mM Hepes pH 7.5, 100mM NaCl, 10mM KCl, 1mM $MgCl_2$ 50 µM DTT, 10% glycerol and 0,1% BSA) and blocked overnight with 5% BSA before incubation with reaction substrates (recombinant tagged proteins plus biotinylated-DOS) for 1 hour at room temperature. Streptavidin beads combined with recombinant sestrins were then washed with PD buffer and proteins were eluted by addition of Laemmli buffer 1x. Followed westernblot assay, proteins were detected with anti-FLAG and anti-Myc antibodies. In parallel, an *in vitro* pull down with DOS-biotinylated was performed directly on $CD4^+$ T cell lysates and presence of Sestrins, p38, JNK, ERK, MIOS and WDR59 was assayed by western-blot.

***In vitro* Kinase Assay**

Purified human senescent $CD28^-CD27^-CD4^+$ T cells and also $sMAC^+$ and $sMAC^-$ $CD4^+$ T cells were lysed in IP buffer (a solution of Hepes (20 mM), NaCl (100 mM), KCl (100 mM), $MgCl_2$ (1 mM), Glycerol (10%) and NP-40 (0.5%) and protease inhibitor (1X)) for 30 minutes on ice followed by centrifugation at 20000g for 30 minutes. The supernatant was then incubated with anti-Sestrin 2 antibody overnight (5 µg). The following day, protein A/G agarose beads (20422; Thermo Scientific) were incubated together with the lysate with anti-sesn2 antibody for 3 hours at 4°C on a rotor. For analysis of the ability of DOS to inhibit MAPK, the immunoprecipitates were treated or not with DOS and ATP (200µM; 9804; Cell Signaling) for 30 minutes at 30°C. The resulting kinase reaction product was then coated in an ELISA plate at 4°C overnight. The plate was then blocked with 5% milk in PBS-Tween 0.5% for 1 hour. To assess the MAPK activity, the plate was incubated for 2 hours at room temperature with one of the following antibodies: anti-p-p38 (1:100), anti-phospho SAPK/JNK (1:100) and phospho-ERK 1/2 (1:100). The secondary anti-rabbit IgG-HRP conjugated antibody (1:500) was

incubated for 1 hour at room temperature. Autophosphorylation within each individual MAPK kinase in the sMAC was derived by subtraction of the corresponding *in vitro* reaction in the absence of ATP. To prove that DOS action is AMPK dependent, the immunoprecipitates were derived from senescent T cells that were depleted or not of AMPK by lentiviral vectors. Ninety-six hours after transduction, T cell extracts were subjected to immunoprecipitation with anti-sestrin antibodies (sestrin 2), then treated with or without DOS and ATP (200 μM) for 30 minutes at 30°C. sMAC activity was assessed with anti-p-p38 antibodies by ELISA after overnight coating on a 96 well plate at 4°C. Alternatively, Compound C (10 μM; 171260; Sigma Aldrich) was added directly to the kinase reaction or to the live cultures of senescent T cells for 2 hours in the presence or in the absence of DOS prior to identical ELISA assays. After overnight blocking (as above), plates were incubated with the primary anti-pp38 antibody (1:100) for 1 hour at room temperature in the dark, followed by incubation with secondary antibody (1:500) 1 hour in the same conditions. For both the assays, TMB substrate was used for detection. Absorbance was detected at 450 nm on a micro-plate ELISA reader (AMR-100, Biolab).

In vitro sMAC disruption

To study sMAC disruption after DOS treatment, AMPK immunoprecipitates obtained as described above were coated on an ELISA plate at 4°C overnight. The plate (wash-in) was then treated with DOS and ATP (200 μM) for 2 hours at 30°C. After the reaction, the wash-out was used to derive wash-out plates by identical overnight coating at 4°C. Wash-in plates and wash-out plates were incubated with anti-sestrin1, anti-sestrin2 or anti-sestrin3 antibodies (1:100) as primary antibodies and detected by ELISA reader following secondary antibody detection. The same experiment was conducted to study sMAC disruption after AMPK inhibition with Compound C; in this experiment the plate was treated with or without Compound C (10 μM) for 2 hours at 30°C, followed by AMPK detection. In some experiments, $sMAC^-$ vs $sMAC^+$ T cell extracts were immunoprecipitated with sestrin 2 or p53 antibodies, to assess respectively sMAC activity or beta-catenin binding, as indicated.

Analysis of sMAC degradation

For the analysis of sestrin2 ubiquitination upon DOS treatment, 5 x10^6 senescent $CD4^+$ T cells were lysed with 100µL of denaturing lysis buffer (a water solution containing SDS (1%), EDTA (5 mM) and β-mercaptoethanol (10 mM)) and boiled for 5 minutes. Samples were then diluted with 900 µl of non-denaturing washing buffer. After lysis, cell extracts were incubated with anti-Sestrin2 antibody (5 µg) at 4°C overnight. In parallel, 200 µl of protein A/G beads were washed 4-5 times in IP buffer and blocked in IP buffer overnight at 4°C. The day after, blocked protein A/G beads were added to the sample and incubated for 3h at 4°C. Protein-beads conjugates were washed with IP buffer and then boiled in presence of Laemmli buffer. Samples were then loaded into polyacrylamide gel and analysed with antibodies to ubiquitinated proteins. For analysis of proteasomal degradation of sMAC, purified human T_{sen} were pre-treated with or without the proteasomal inhibitor MG132 (10 µM; M7449; Sigma-Aldrich) for 30 minutes at 37°C, prior to DOS exposure for 2 hours in culture. Cells were then lysed as described above and analysed by direct immunoblotting for sestrin2 and AMPK.

AMPKγ-ATP loading assay

Recombinant AMPK γ1 chain (AMPKɣ; AR51158PU-S, OriGene) and Sestrin 2 (GWB-66FAFC50UG, Aviva) were diluted in IP buffer (Hepes 20 mM, NaCl 100 mM, KCl 100 mM, $MgCl_2$ 1 mM, 10% Glycerol) at a final concentration of 5 µg/ml and 20µg/ml respectively. ATP (200 µM) was used in the reaction. For IP loading, AMPKɣ was immunoprecipitated with Anti-His tag monoclonal antibody (TA100013, OriGene) after 5 minutes of *in vitro* reaction at 30 °C. Reaction volume was 50µl.

In order to follow in the window of the ATP detection, the samples were serial diluted with dilution buffer in the range 10^{-6} to 10^{-12} M. ATP was detected using the ATP Bioluminescence Assay Kit (HS II-11 699 709 001-Roche) following the manufacturer's instructions. Luminescence was acquired at the Varioskan LUX Multimode Microplate reader (ThermoFisher).

Fluorescent ATP-binding detection

5μM of recombinant total AMPK (P47-110GH-10; Signal Chem) was mixed with 20μM of recombinant sestrin 2 (Genetex) according to the stoichiometry ratio 1:4. In parallel, recombinant AMPKγ protein (5μM; AR51158PU-S, OriGene) was mixed with 20μM of sestrin (Genetex). Condition without sestrin was used as control. The binding reaction was carried out in 50 μl of TrisHCl buffer (10mM; PH8); incubated at 30°C for 5 minutes in presence or in absence of DOS. After this time, 10μM of MANT-ATP (NU-202S; Jena Bioscience) was added to each reaction and the released fluorescence was quickly registered at 448nm. Fluorescence signal is proportional to the amount of ATP-bound at the AMPK CBS sites (1 and 3). Addition of 200μM of ATP post MANTATP binding disrupted MANT-ATP fluorescence confirming ATP binding.

Sestrin-AMPK binding strength assay

Human T_{erl} cells were treated with A-769662 (AMP-activated protein kinase activator, ab120335) at 100 μM and incubated for 3 days. After this time, cells were lysed and total AMPK protein was immunoprecipitated with the antiAMPKα antibody (2532S, Cell Signaling). Fifty ng/well of the T cell immunoprecipitates were coated into an ELISA plate and incubated at 4 °C overnight. The plates were then blocked with 4% milk in PBS-Tween 0.5% for 1hour before adding recombinant Sestrin 2 (50 ng/μl) for 2 hours at 30°C. After this time, urea (3M; 57-13-6, Merck Millipore) was added for 10 minutes to break the AMPKSestrin2 binding followed by incubation with the anti-Sestrin2 antibody (1:100, #8487, Cell Signaling) and secondary anti-rabbit IgG-HRP conjugated antibody (1:500). TMB substrate was used for detection. Absorbance was detected at 450 nm on a micro-plate ELISA reader (AMR-100, Biolab). In some experiments, the immunoprecitates were incubated with exogenous sestrin, washed and then analysed for binding strength with or without Urea at various concentration (3M or 6M), to monitor interaction strength.

Molecular docking simulations

To predict the potential binding site(s) of DOS46L to Sestrin-2, protein-peptide molecular docking was performed using AutoDock Vina 1,2. As the available Sestrin-2 crystal structures in Protein Data Bank do not have a complete defined tertiary structure (PDB code: 5CUF; 5DJ4; 5T0N; 6N0M), structure prediction of Sestrin-2 was fetched from AlphaFold Protein Structure 3 Database. Sestrin-2 structure was then optimized for docking, using Dock Prep tools by UCSF Chimera 4. Briefly in this step, hydrogen atoms were assigned and gasteiger charges and net charges were calculated. Processed Sestrin-2 structure was saved in a PDB file. The 3D-structure of DOS 46L was then generated by CycloPs 5, a GUI python program for building cyclic peptide structures from peptides sequences. Energy minimization and optimization for docking were performed in UCSF Chimera, similarly to Sestrin-2 optimization/following the steps of Sestrin-2 optimization. Optimized structure of DOS 46L was saved in a Sybyl Mol2 file for docking. After protein and ligand preparation, AutoDock Vina with default parameters was used. Models of the complexes of DOS46L interacting with Sestrin-2 were obtained and UCSF Chimera was used to plot the modelling figures.

Generation of DOS disruption sestrin mutants

Sestrin-a (436T-A; 306P-A) and b (94W-A; 74G-A) mutants and wild type constructions were cloned into pDUAL-PuroR, pDUAL-BlastR and pDUAL-PuroR vectors under the transcriptional control of the spleen focus-forming virus (SFFV) promoter by standard cloning techniques. GFP, Puromycin (PuroR) and Blasticidin (BastR) resistance genes were expressed under the transcriptional control of the ubiquitin promoter WPRE and CPPT sequences present in the pDUAL vector increase transgene expression system. Standard cloning techniques were followed. Briefly, sestrin-a and b mutants were first amplified on KanR cloning plasmids, then the plasmid was digested by BamHI-NotI 10U/μL (Thermo Fisher Scientific) restriction enzymes in Fast Digest Buffer for 1hour at 37ºC to purify the transgene of interest. Wild type sestrin construction was generated inserting the AatII-NotI fragment of the b construct into the a construct to eliminate mutations. AatII-NotI (10U/ul) enzymatic digestion was

conducted in Fast Digest Buffer for 1hour at 37ºC to purify the transgene of interest. Fragments were purified by Qiagen cloning standardized protocol and ligated to the pDUAL of interest by the T4 ligase enzyme (Promega) for 1 to 24 hours at room temperature. Ligations were transformed into Echerichia coli XL/1 Blue competent bacteria and the DNA of interest was purified by miniprep. Then, the positive minipreps were transformed into Echerichia coli XL/1 Blue competent bacteria the DNA of interest was purified by midiprep. Qiagen cloning standardized protocols were followed. DNA concentration was measured by Nanodrop spectrophotometer. The size of the purified plasmid was analised by electrophoresis in 1.5% agarose gel (1.5% agarose, RedSafe™ Nucleic Acid Staining Solution (20,000x) (iNtRON) in the TAE 1X buffer). To verify the correct structure of the plasmids, the purified DNA was digested with the restriction enzymes BamHI-NotI 10U/µL (Thermo Fisher Scientific), or with HindIII in Fast Digest Buffer (Thermo Fisher Scientific) for 1 or 2 hours respectively, at 37ºC. The product of digestion was run in 1.5% agarose gel. It was verified that the sizes of bands obtained were as expected. All insert sequences were confirmed by Sanger Sequencing.

Lentivirus production and purification

At day 0, HEK293 T cells (CRL-11268; ATCC) were plated in T75 flasks. The day after, cells (70% confluent) were transfected with 10µl Lipofectamine LTX (15338100; ThermoFisher) combined with PLUS reagent in a ratio 1:1 and 4µg of DNA with the following three plasmids: pCMV-VSV-G envelope vector (RV-110; Cell Biolabs); p.891 packaging vector; p-SIREN-scramble/p-SIRENshsesn1/ p-SIREN-shsesn2/ p-SIREN-shsesn3[2] , 48 and 72 hours later, supernatants from transfected HEK293 T cells containing lentivirus were collected. Lentiviral particles were then concentrated according to Lenti-Pac Lentivirus Concentration Solution protocol (LT007; GeneCopoeia).

Cell trace violet (CTV) staining in sestrin null senescent T cells

One million of purified human $CD4^+$ T_{sen} was activated with an anti-CD3 antibody coated-plate (0.5µg/ml) plus rhIL-2 (5 ng/ml; 11 011 456 001; Sigma). Forty-eight hours post-activation, cells were

transduced with p-SIREN-sh lentivirus particles to target sestrins or with the control p-SIREN scramble at a multiplicity of infection (MOI) of 10. Ninety-six hours after transduction, cells were treated with 5 μM of Cell Trace Violet Cell Proliferation Kit (C34557; ThermoFisher), incubated for 10 minutes at 37°C, then washed and resuspended in media in the presence or not of DOS. Cells were then cultured for additional 3 days and re-activated as above, followed by CD3 and CD28 staining, and CTV dilution detection. Gating was performed among the GFP^+ effectively transduced population (reporter gene) and analysed at the CytoFLEX flow cytometer.

CTV in shAMPK DOS treated senescent T cells

Purified human $CD4^+$ T_{sen} cells were transduced with lentiviral vectors containing shScramble (as control) or shAMPKα siRNA expression construct and maintained in culture for 21 days. Cells were activated every ten days with anti-CD3 antibody and recombinant rhIL-2, as above. After one month of culture, cells were treated with DOS and stained with 5 μM Cell Trace Violet, then reactivated for additional 3 days. CTV Analysis on transduced GFP^+ T cells was then performed at the cytofluorimeter.

***In vitro* BrdU proliferation assay**

Purified human $CD4^+$ T_{sen} cells were stimulated for 48 hours with anti-CD3 antibody (0.5μg/ml) plus rhIL-2 (10 ng/ml), then transduced with shSestrin1/2/3 lentiviral vectors as previously described[2]. Ninety-six hours post-transduction, senescent $CD4^+$ T cells were treated with BrdU (5-bromo-2′deoxyuridine; 10μM; B23151-ThermoFisher) for 72 hours; then permeabilized and stained with antiBrdU primary antibody (1:100; ab6326; Abcam) to assess proliferation by flow-cytometry. In some experiments, $CD4^+$ T_{sen} cells were cultured as above described for 3 days and cell cycle progression was measured by propidium iodide incorporation according to the manufacturer's instruction (Abcam, Ab139418). Cell cycle progression was further assessed measuring levels of cell cycle suppressors (p21) and cyclin D1, as previously described[1].

β-galactosidase staining

Purified T_{sen} were cultured for one week in a plate coated with anti-CD3 antibody (0.5 μg/ml) with the addition of rhIL-2 (5 ng/ml), in absence or not of DOS. One week later, $2*10^5$ cells were transferred on poly-lysine coated 96 well plates and stained using Senescence β-Galactosidase staining kit, following the manufacturer's protocol (9860; Cell Signaling Technology). Cells were then imaged on a Zeiss-Primovert inverted phase-contrast microscope.

AnnexinV staining

For analysis of cellular toxicity, human $CD4^+$ T cells were treated with DOS, H_2O_2 (500mM; positive death control) or left untreated. Cells were stained using the Annexin V-FITC Apoptosis detection Kit (ab14085; Abcam) following the manufacturer protocol. Annexin levels were acquired by flowcytometry. Annexin V staining was used also for detection of dead cells in CD45.1 mice adoptive transfer experiments.

Seahorse assay for cell metabolism

To measure fatty acid oxidation, purified $sMAC^-$ *vs* $sMAC^+$ $CD4^+$ T cells were activated with anti-CD3 antibody (0.5 μg/ml) plus rhIL-2 (5 ng/ml) and treated overnight with or without DOS. The day after, the media was replaced with XF Base Medium Minimal DMEM (103334-100; Agilent) composed of basic DMEM plus 0.5 mM glucose, 1 mM glutamine and 1% FBS. Cells were incubated with this media for 4 hours before plating with the assay media (composed of XF Base Medium Minimal DMEM supplemented with 2 mM glucose and 0.5 mM L-carnitine; Agilent) in the XF96 well plate (Agilent) pre-treated with poly-lysine at $2*10^5$ cells/well. Cells were then incubated for 1 hour at 37ºC without CO2. Just before the assay, cells were treated with 1X palmitate-BSA or with 1X BSA. According to the Palmitate Oxidation Stress Test protocol (Agilent), during the assay, cells were treated at different time points with Etomoxir (4 μM; 103672-100; Agilent), Oligomycin (1.5 μM; 103672-100; Agilent),

FCCP (1 μM; 103672-100; Agilent) and Rotenone/Antimycin A (0.5 μM; 103672-100; Agilent). OCR values were acquired by Seahorse Machine (XFe96) over a time of 120 minutes.
For fatty acid oxidation, subtraction of etomoxir treated conditions was used to derive lipid burning as recommended by the manufacturer (Agilent). In some experiments, to further confirm DOS specificity of action, metabolic assessment was performed in human sMAC$^+$ CD4$^+$ T cells that had been shRNA-depleted, or not, of all sestrins prior to overnight DOS treatment.

Yellow fever specific T cell stimulation

Purified human CD4$^+$ T cells were pre-treated with or without DOS for 4 hours; in parallel, autologous APCs were preloaded with or without yellow fever vaccine (1:200 of the human dose, Stamaril; Sanofi Pasteur) or specific YF peptides (2ug/ml: PepMix YF- NS4B; Innovative Peptide Solutions). In control experiments, APCs were loaded with negative control peptides (2ug/ml PepMix Human-Actin; Innovative Peptide Solutions). T cells and antigen-pulsed APCs were then co-cultured for 18 hours, in a 1:2 ratio. The next day, cells were treated for 4 hours with Brefeldin A (1 μg/mL; Sigma-Aldrich). CD4$^+$ T cells stimulated for three hours with PMA (50 ng/ml) and ionomycin (1 ug/ml) were used as a control. Cells were stained for CD3, CD4, CD28, CD45RA, CD95, CD62L, and for intracellular TCF1 and IFN-γ detection. Antigen specific events were derived by subtraction of the unstimulated background, with or without DOS. Analysis was carried out by flow cytometry.

TREC investigation

For polyclonal analysis of human TCR recombination, purified human CD4$^+$ T cells were plated overnight, for 3 days, or for one week with CD3/CD28 Dynabeads, in the presence or not of DOS.
For antigen specific TCR recombination instead, human CD4$^+$ T cells were pre-treated with DOS for 4 hours and APCs pre-loaded with YF peptides (2ug/ml; PepMix YF- NS4B; Innovative Peptide Solutions) for the same time. The T cells were then co-cultured to allow synapse formation with APCs, in a 1:2 ratio. Antigen-specific TRECs were analyzed 18 hours later by background subtraction of

antigen free immune conjugates with or without DOS, as above described. For both experiments, DNA was isolated following TRIzol reagent protocol (15596018; ThermoFisher) and quantified with NANO-DROP spectrophotometer (Thermo-Scientific). qPCR was performed with 100 ng of gDNA, 900nM primers, 250nM TaqMan probe per sample according to the SensiFAST Probe Hi ROX kit (BIO-82005 Bioline).

To investigate TRECs, the following primers were used:

Fw CACATCCCTTTCAACCATGCT

Rw GCCAGCTGCAGGGTTTAGG

Probe [6FAM] ACACCTCTGGTTTTTGTAAAGGTGCCCACT [TAM]

The qPCR reaction was conducted by using !StepOne Plus System" machine (Applied Biosystems).

For analysis of mouse TCR recombination, murine $CD4^+$ T cells were purified from peripheral lymphoid organs of mice treated or not with DOS. Cells were left to rest in culture overnight and the day after they were assayed for the TREC expression according to the above described procedure for human TREC investigation. For mouse TRECs, the following specific primers were used:

Fw CCAAGCTGACGGCAGGTTT

Rw AGCATGGCAAGCAGCACC

Probe [6FAM] TGCTGTGTGCCCTGCCCTGCC[TAM]

The same procedure was used to measure TRECs in $CD45.1^+$ $CD4^+$ adoptively transferred T cells in CD45.2 recipients.To investigate how TREC production could be affected by depletion of Rag proteins, 2 millions of purified $CD4^+$ T cells were electroporated in the presence of siRNA for RAG1 (sc-42962; SantaCruz) and RAG2 (sc-36371; SantaCruz). siRNA scramble (sc-44236; SantaCruz) was used as control. Electroporation was performed according to the Human T cell nucleofactor kit protocol (Lonza) as previously described (13). Cells were left for 60 hours in culture post electroporation with exposure or not to DOS for the remaining 4 hours of silencing prior to conjugation with autologous YF pulsed APCs, in a 1:2 ratio. For APC antigen loading, YF peptide mix was used (2ug/ml; PepMix YF- NS4B; Innovative Peptide Solutions). In parallel, conjugates were left unstimulated with or without DOS. After

the overnight coculture, $CD4^+$ T cells were purified and genomic DNA was extracted according to TRIzol reagent protocol (15596018; ThermoFisher). The DNA was quantified with NANO-DROP spectrophotometer (Thermo-Scientific). TREC levels were investigated by qPCR according to the protocol above described. Antigen specific TRECs were derived subtracting the raw data originated from unstimulated cultures with or without DOS, to identify the events occurring specifically in response to the DOS when combined with the YF peptides, or any YF specific events without DOS respectively.

TCR Sequencing

Human APCs and $CD4^+$ T cells were purified from PBMCs. Six million APCs were preloaded with YF peptides (2ug/ml; PepMix YF- NS4B; Innovative Peptide Solutions) or left unstimulated for 4 hours and then co-cultured with three million $CD4^+$ T cells that had been pre-treated or not with DOS for the same time. In parallel donor matched cultures, EBV peptides (1:50; peptivator EBV consensus;) were used instead of YF. After the overnight co-culture, $CD4^+$ T cells were purified and genomic DNA was extracted according to the "PureLink DNA mini kit" (Invitrogen). DNA concentration was acquired at the NanoDrop spectrophotometer (ThermoFisher). This experiment has been performed in parallel in four donors to have biological replicates. DNA samples were sent out for direct *TCR*b sequencing. *TCR*b amplification was carried out according to Robins et al. (2009)[4] by using Qiagen Multiplex PCR kit and the reported primers. The method is capable to detect unique TCR repertoire, including the rarest receptor sequences. For indexing, KAPA HiFi HotStart ReadyMix (Roche) and Dual Index Set (NEB) were used. The libraries were sequenced on an Illumina MiSeq platform using 2x250bp paired-end sequencing with a coverage of ten million reads. Fastq files were first subjected to quality control using FastQC (v0.11.9)[5]. TCR repertoire analysis and error correction were then performed using MiXCR (v4.2.0)[6]. Filter for low quality reads and adapter trimming was further performed using trimmomatic software (v0.39). Plots such as heatmaps were generated using the R programming language[7, 8]. In addition, individual VDJ clonotypes and clonotype usage, as well

examples of unique *de novo* antigen-specific clonotype formation are also shown across all conditions. Software generated VDJ tools (Java V1.2.1) were used for clonotype analysis.

TRBV clone validation

Donor-matched YF-specific conjugates were formed as above described ("**Yellow fever specific T cell stimulation**") for 18 hours, in the presence or in the absence of DOS. The day after, cells were treated with brefaldin A (1:1000; Sigma-Aldrich) for 4 hours. Cells were stained for the surface proteins CD4, CD28, CD45RA, CD62L, CD95, and intracellularly, for TCF1 and IFN-γ, as indicated. In addition, expression of donor-matched YF-specific TCR variants identified during Next Generation TCR Sequencing was validated by flow cytometry with variant specific antibodies to TCRvβ2, 7.1, 14, 16 and 17. For the mouse side, TCR rearrangements were assessed in $CD4^+$ T cells purified from lymphoid organs of old mice treated or not with DOS and then infected or not 2 months later with H1N1 virus($3.5*10^5$ PFU). Cells from young mice infected with the same virus were used as control. All mouse T cells were stained for the surface TCR variants vα8.3 and vβ12, previously reported to be associated with the anti-Flu response[9]. For the purification of individual TRBV clones, NGS-matched human $CD4^+$ T cells were pre-treated with or without DOS then co-cultured with autologous APCs pre-loaded with YF-vaccine or peptides for 18 hours, as indicated. Post-synaptic $CD4^+$ T cells were then gently detached from the conjugates using a 2 ml syringe with cold PBS and processed for sorting. For cell sorting, post-synaptic $CD4^+$ T_{STEM} were stained with antibodies directed to CD45RA, CD28, CD95 and CD62L surface markers in combination with a single TRBV clonotype antibody as follows: $TCRvβ2^+$, $TCRvβ7.1^+$, $TCRvβ14^+$, $TCRvβ16^+$, $TCRvβ17^+$. In parallel, T_{EM} and T_{CM} for each TCRvβ clonotype were also sorted based on the relative expression of CD45RA and CD28 surface markers. Cells were sorted with a MoFlo Astrios-EQ flow cytometer (Beckman Coulter). Isolated TRBV clones ($2*10^5$ each) were then rested for 5 days followed by re-stimulation with YF peptide (2 ug/ml) or YF-vaccine (1:200 of the human dose) for 18 hours. Cell supernatants were assessed with Human IFN γ ELISA Kit (abcam; ab46025) according to the manufacturer's instructions. T_{EM} and T_{CM} IFNγ supernatants were measured

as negative controls. To assess YF-specific TRBV T_{STEM} clone proliferation, $CD4^+$ T_{STEM} ($2*10^5$ each) from every TCRvβ clonotype subset that had been derived and sorted as above were incubated with BrdU labeling solution for 4 hours, followed by re-challenging with autologous YF-pulsed APCs for additional 4 days. TCRvβ $CD4^+$ T_{STEM} cells were tested with the BrDU Cell proliferation ELISA kit (abcam; ab126556) according to the manufacturer's instructions. Sorted TCRvβ T_{EM} and T_{CM} were tested in parallel as negative controls.

In some experiments, Donor-matched YF-specific conjugates were formed as previously described ("**Yellow fever specific T cell stimulation**") for 18 hours, in the presence or in the absence of DOS; except that CD4+ T cells were blocked with anti-CD40L antibody for 30 minutes before the co-culture with APCs to avoid CD40L degradation[10,11]. The day after, cells were treated with brefaldin A (1:1000; Sigma-Aldrich) for 4 hours. Cells were stained for the surface proteins CD4, CD28, CD45RA, CD62L, CD95, CD69, CD40L, TRVB 7.1. AIM cells were defined as CD69+ CD40L+ among the TRBV expressing stem T cells.

Telomere live transfer

Ten million of purified human APCs with live labelled telomeres were allowed to form synapses with autologous T_{sen} (3:1 ratio) in the presence or in the absence of DOS and stimulated overnight with a 1:1 mix of CMV and EBV antigens (Peptivator CMV pp65 130-093-438 and Peptivator EBV Consensus 130-099-764; Miltenyi). The day after were stained for CD3, CD4, CD27, CD28 receptors and analysed by flow-cytometry for transferred APC telomere fluorescence into recipient T cells[12].

Telomere Length Quantification Assay

Purified human APCs ($4*10^6$) and T_{sen} ($1*10^6$) were conjugated with CMV and EBV antigens (3:1) and treated or not overnight with DOS. The day after, cells were detached from conjugates with a 2ml syringe and cold PBS. After a $CD4^+$ T cell purification as above described, genomic DNA was extracted

from senescent T cells according to PureLink Genomic DNA Mini Kit protocol (K182001; Invitrogen). qPCR reaction was performed in the extracted DNA according to the protocol suggested by the "Absolute human telomere length quantification qPCR Assay kit" (8918; ScienCell Research Laboratories). Telomere length was calculated from the ΔCT, according to the formula suggested by the kit.

Telomerase Activity

$CD4^+$ T_{sen} were purified from human PBMCs. Purified T_{sen} were plated in an anti-CD3 coated plate in the presence of IL-2 (5ng/ml) and left in culture for 72 hours with or without DOS. Cell pellets from the three different cell types were assayed for telomerase activity according to the TeloTAGGG Telomerase PCR ELISA Kit (11854666910; Roche).

DOS_{juv} $CD4^+$ T cell Adoptive transfer

Twenty months old mice (C57BL/6 wild type CD45.1) were primed with Fluad (1:20 of the human dose; Seqirus) and subcutaneously injected with or without DOS (0,1mg/Kg). After 15 days, mice were culled and peripheral lymphoid organs collected. Splenic donor $CD4^+$ T cells were purified, stained with CTV and phenotype before injection into young naïve congenic recipients (3 months). Mice not receiving donor cells were used as negative transfer control. Twenty-eight days later, mice were sacrificed, organs collected and CTV^+ cells analyzed at the CytoFLEX flow cytometer. Alternatively, aged-matched CD45.1 mice (20 months) from vaccinated donor animals were derived as above described and injected without CTV labelling into CD45.2 young recipients (3 months) to allow tracking after transfer independently of CTV. No vaccination of recipients was performed in either protocol, with similar results. Ten million or 5 million cells were used for adoptive transfer, with similar results, as indicated. To study the role of $CD4^+$ T cells on driving DOS effects, old CD45.1 mice (20 months) were injected or not with DOS. Seventy-two hours later animals were culled and $CD4^+$ T cells were isolated from their spleens and then intravenously injected into aged-matched CD45.2 recipient mice

($5x10^6$ $CD4^+$ T cells per mouse). Vaccination with Fluad was performed or not 24 hours after transfer as indicated below. Eight weeks later, all mice were exposed to the H1N1 flu virus ($5x10^5$ PFU) and then daily monitored for the next 15 days. During this period, clinical parameters were acquired: fur condition, posture, movement, breathing, eye state, and weight loss to assess a clinical score.

Once reached a total score of 13 or more, mice were humanely euthanized accordingly to the animal ethical guidelines; animals with good parameters were instead euthanized 15 days post infection. Several tissues (blood, lung, spleen, and lymph-nodes) were collected from all the animals for further analysis.

Experimental mouse groups:

- 5 old CD45.2 mice (20-month-old) receiving age-matched DOS_{juv} $CD45.1^+$ $CD4^+$ donor T cells and vaccinated with Fluad.
- 5 old CD45.2 mice (20-month-old) receiving age-matched $CD45.1^+$ $CD4^+$ donor T cells (DOSfree) and vaccinated with Fluad
- 5 old CD45.2 mice (20-month-old) receiving young $CD45.1^+$ $CD4^+$ donor T cells and vaccinated with Fluad
- 5 old CD45.2 control mice (20-month-old) transfer free injected with vehicle and vaccinated with Fluad
- 5 young CD45.2 mice (3 month old) transfer free injected with vehicle and vaccinated with

Fluad without DOS

- 5 old CD45.2 mice (20 month old) receiving age-matched DOS_{juv} $CD45.1^+$ $CD4^+$ donor T cells without vaccination.

sMAC expression in human T cells

Purified human $CD4^+$ T cells were stained for the surface proteins CD4, CD28, CD45RA receptors and for the intracellular proteins sestrin 2 and phopsho-p38 directly *ex vivo* and analysed by cytofluorimetry. sMAC expressing cells as considered as sestrin and p-p38 positive populations.

***In vitro* antigen-specific IgG production**

PBMCS were treated with or without DOS then cultured for 14 days with Fluad vaccine (1:50 human dose; Seqirus). In some experiments, human $CD4^+$ T cells were depleted from the immune cultures by magnetic isolation prior to Fluad stimulation, to assess impact of these cells on the vaccine response upon DOS treatment. Fluad vaccines (1:40 of the human dose) were coated on 96 wells overnight at 4°C and then blocked with 4% milk in PBS 0.5% Tween-20, 2 hours at room temperature. 100ul of supernatant was then added and left incubating overnight at 4°C. Negative controls were coated with PBS 1X instead of Fluad vaccine and used as background throughout. Furthermore, in parallel coating, unvaccinated serum was used as further negative control for presence of unrelated IgGs. The plate was washed and then incubated with anti-mouse IgG1 biotin conjugated antibody (1:250; 130-095-879; Miltenyi) for 2 hours at room temperature. After washing and incubation with streptavidin-HRP conjugated antibody (1:3000; 1610381; Biorad) for 1 hours at room temperature, TMB substrate was added. The reaction was stopped with the stop solution. The absorbance was detected at 450 nm at the ELISA micro-plate reader (AMR-100, Biolab).

RNA extraction, retro-transcription and qPCR

Total RNA from $CD4^+$ T cells purified from mouse spleen, lymph nodes or lung cells was extracted using the “PureLink RNA Mini Kit” (12183018A; Invitrogen). The RNA concentration was acquired by NANO-DROP spectrophotometer (Thermo-Scientific). One µg of total RNA was retrotranscribed to cDNA following the protocol advised from the “qScript cDNA synthesis kit” (733-1174; Quantabio). qPCR reaction was performed with 100 ng of cDNA per sample using the kit SensiFAST SYBR Hi ROX kit (BIO-92005; Bioline).

For investigation of mouse *sestrin 2* the following primers were used:

Fw TCTCGGCACTTTGAGGACAC

Rw AACCATGGTCTTCCCAGCAG

In parallel, to investigate the expression levels of other genes of interest, the TaqMan approach was used. In this context, qPCR reaction was performed with 100 ng of cDNA per sample using the kit SensiFAST Probe Hi ROX kit (BIO-82005; Bioline). The expression of *IL7RB* was assessed with the TaqMan probe Mm00434295 (ThermoFisher), while for the house-keeping gene, β-*actin*, the probe Mm02619580 was used (ThermoFisher). To investigate the presence of the H1N1 virus in the lung of infected mice, total DNA was purified from the tissue according to the TRIzol reagent protocol (15596018; ThermoFisher), quantified and amplified for the PA viral gene of H1N1 virus with the following primers:

Fw CGGTCCAAATTCCTGCTGA

Rw CATTGGGTTCCTTCCATCCA

The following primers were instead used to amplify the house-keeping gene, *RPL34,* used as control:

Fw GGTGCTCAGAGGCACTCAGGATG

Rw GTGCTTTCCCAACCTTCTTGGTGT

For investigation of DOS driven Rag re-expression, we used RAG1 Human qPCR Primer Pair (NM_000448; #HP200428, Origene) AND RAG2 Human qPCR Primer Pair (NM_000536; #HP200508, Origene).

All qPCR reactions were conducted by using “StepOne Plus System” machine (Applied Biosystems).

Chromatin Immune Precipitation (Chip)

For detection of murine HDAC1 activity, chromatin was immunoprecipitated from peripheral lymphoid organs of old mice (20 months) treated or untreated with DOS and from their young controls. All mice were H1N1 infected 2 months after DOS treatment (DOS only protocol, see above). Chip was performed using Pierce™ Chromatin Prep Module kit according to the manufacturer's instructions with anti-HDAC1 antibody. The Chip reactions were then incubated for 1 hour at 30°C with an exogenous DNA purified from peripheral lymphoid organs of naïve old mice (20 months). HDAC1 activity was measured by ELISA assay detecting the level acetylated Histone 3 (anti-acetil-H3; K27; 8173S; Cell Signaling). For detection of DNA-bound B-catenin (activated) chromatin was immunoprecipitated with anti-b-catenin antibody from purified $sMAC^-$ and $sMAC^+$ T cell populations as above described treated or not with DOS for 4 hours.

Sestrin 2 gene acetylation

To investigate epigenetic changes induced by DOS treatment *in vivo,* the chromatin was immuneprecipitated from peripheral lymphoid organ cells of old mice treated or untreated with DOS and from their young controls following the manufacturing protocol of the Pierce Chromatin Prep Module kit (26158; Thermo Scientific). *Sestrin 2* gene is mainly acetylated at histone 3, for this reason an anti-histone 3 antibody (anti-acetil-H3; K27; 8173S; Cell Signaling) was used for the immuneprecipitation. The antibody anti-5 methylcytosine was used in parallel as control. After DNA purification *sestrin 2* expression was assessed by qPCR with primers specific for the mouse sestrin 2. The following primers were used:

Fw AGGAGTGTCTATCGCCGTAGCG

Rw TGGGACACCCGAGGGGTCTAGGT

qPCR reaction was performed using the kit SensiFAST SYBR Hi ROX kit (BIO-92005; Bioline) on a "StepOne Plus System" machine (Applied Biosystems).

DOS kinetics

Mice (strain C57BL/6) were divided in 2 groups:

1. 5 old mice (18-month-old) injected subcutaneously with DOS 46L at 0.1mg/kg
2. 5 old mice (18-month-old) control subcutaneously injected with vehicle 3. 5 young mice (3-month-old) control

Mice were bled at 48, 72, 96 hours and 10 days post injection. Sestrin2 levels were monitored by flow-cytometry.

Mouse Survival

C57BL/6 mice were subcutaneously injected with Fluad vaccine (1:20 human dose; Seqirus) and divided in the following groups:

- 7 old mice (18-month old) vaccinated with Fluad without DOS
- 8 old mice (18-month old) vaccinated with Fluad + DOS 46L (0,1 mg/Kg)
- 7 young mice (3-month old) vaccinated with Fluad without DOS

Six months post vaccination, mice were then infected with H1N1 flu virus ($6*10^5$ PFU) and then monitored for the following 15 days: body weight, disease progression, clinical score and survival data were acquired. After 15 days, mice were sacrificed and tissues were collected (blood, lung, spleen and thymus). Clinical score included: fur condition, posture, movement, breathing, eye state, and weight loss according to ethics and under veterinary supervision. Animals were sacrificed when reaching a clinical score of 13 or above (grade of severity accepted from the ethic commission), or in any case of severe dyspnea.

Determination of antigen specific IgG production *in vivo*

Identification of IgGs levels on mouse plasma was performed at 18, 36 days and 8 weeks after mouse immunisation with Fluad vaccine (1:20 of the human dose; Seqirus) by ELISA assay as above described. For viral specific antibodies, H1N1 live particles were used for coating instead of Fluad. IgGs were

investigated at the same way in mouse blood of the DOS-juvenated adoptive $CD4^+$ T cell transfer experiment.

Micro-neutralization Assay

Mouse heat-inactivated sera were diluted 1:200 and pre-incubated with H1N1 virus (1:10000 dilution) for 1 hour at 37°C. MDCK cells (CCL-34; ATCC) were added to sera-viral mix at concentration of 15.000 cells per well (96 well plate) and incubated overnight at 37°C. The following day, cells were first fixed with cold Acetone 80% in PBS and then incubated for 1 hour at room temperature with anti-influenza A NP antibody (1:250; ab20343; Abcam). Secondary antibody was goat anti-mouse IgG HRP labelled (1:2500; Millipore). The reaction was developed by ELISA as above. Percentage of death inhibition was calculated setting the OD450 value of positive dead cell control as 0% and OD450 value of negative null death as 100%.

Mice treated only with DOS and infected with H1N1 virus

C57BL/6 mice were divided in the following groups:

- 10 old mice (18-month old) treated with DOS46L (0.1mg/kg)
- 10 old mice (18-month old) not injected with DOS
- 10 young mice (3-month old) not injected with DOS

Mice were intra-nasally infected with H1N1 viral particles ($3.5*10^5$ PFU) either 48 hours (immediate infection) or 8 weeks (delayed infection) after subcutaneous DOS administration (0.1 mg/Kg). Mice were monitored for 15 days and clinical score parameters were recorded: fur condition, posture, movement, breathing, eye state, and weight loss. Animals were sacrificed according to clinical score threshold of 13 or in any case of severe dyspnea, as above. Tissues were collected from each mouse (blood, lung, spleen, lymph-nodes and thymus).

Adoptive transfer for B cell phenotype

Twenty-month-old mice (CD45.1 C57BL/6 strain) were subcutaneously injected or not with DOS. After 72 hours, mice were culled and spleens were collected; CD45.1 $CD4^+$ T cells and all other immune cells depleted of $CD4^+$ T cells were purified. Complete $CD4^+$ T cell depletion was confirmed into the $CD4^-$ T cell pool by flow-cytometry. Each CD45.2 recipient mouse received $5*10^6$ of purified CD45.1 $CD4^+$ T cells or $CD4^-$ cells via caudal vein injection. Young $CD4^+$ T cell from naïve animals were also transferred. Young and old and DOS treated mice, free of transfer, were used as control. The day after transfer, CD45.2 recipient mice were subcutaneously vaccinated with Fluad (1:20 of the human dose). Fifty-teen days later, recipient mice were bled to investigate Fluad specific IgGs, before proceeding with animal sacrifice and collection of the peripheral lymph nodes. B cells from lymph nodes were stained for the following cell surface markers: CD19, CD45R (B220), CD138, GL7. $CD3^+$ $CD4^+$ and $CD3^+$ $CD8^+$ T cells were excluded from gating.

For IgG1 quantification, a standard curve was obtained with well-defined recombinant IgG1 protein (ab180055; abcam) concentrations and compared against IgG1-containining mouse sera from vaccinated animals, run in parallel.

***In vitro* B cell phenotype**

$CD4^+$ T cells were derived from twenty-month old mice (C57BL/6 strain) and stimulated for 48 hours with CD3/CD28 Dynabeads (11452D, Gibco). The cells were then transduced with p-SIREN-sh lentivirus particles to target sestrins or with control p-SIREN scramble vectors, at a multiplicity of infection (MOI) of 10. After 72 hours, the transduced $CD4^+$ T cells were cultured with autologous purified APCs in a 1:2 ratio. The co-cultures were stimulated with Fluad vaccine (1:100 of the human dose) and treated or not with DOS. After 10 days of culture, B cells were stained for the following surface proteins CD19, B220, CD138, CD38. T cells were excluded by gating out $CD3^+$ $CD4^+$ $CD8^+$ lymphocytes.

Cytokine production and T cell subpopulation induction in splenocytes

For the antiviral response, T cells from DOS only treated, H1N1 infected mice were re-exposed to H1N1 viral particles and Th1 state was analyzed 3 days later for the intracellular IFN-γ and Tbet expression among $CD3^+$ $CD4^+$ T cells. Young mice were used as control. The same approach was used to investigate CD45.1 Th1 response in the DOS-juvenated adoptive $CD4^+$ T cell transfer among CD45.2 recipient lymph nodes or lungs, as indicated. Tfh were detected among $CD45.1^+$ $CD4^+$ T cells subjected to adoptive transfer in old CD45.2 recipients and analysed 15 days after recipient Fluad vaccination. Cells were stained for CD3, CD4, CXCR5 and PD1 markers.

IFNγ production in response to Yellow Fever in mouse splenocytes

Induction of *de novo* YF specificity was further proved in OT-II transgenic mice that only respond to OVA. T cells were derived from OTII splenocytes and challenged with YF pulsed APCs in the presence or in the absence of DOS for 18 hours. The day after, stem T cells were purified by FACS sorting, rested for 5 days and re-challenged with APCs loaded with YF peptides (2ug/ml; PepMix YF- NS4B; Innovative Peptide Solutions). IFN gamma release was measured in the culture supernatant by ELISA (ab100689; abcam) 18 hours later. Positive control IFN gamma T cell release derived from OVA immunised animals, whose OT II $CD4^+$ T cells were re-challenged with OVA *in vitro* 15 days after vaccination.

Statistical analysis.

A maximum of nine (human experiments) or 10 (mouse work) biological replicates for each experiment, with at least of three independent biological replicates throughout, as indicated. GraphPad Prism v9 was used to perform statistical analysis. For pairwise comparisons in human experiments, a two-tailed, paired Student's t-test was used. For pairwise comparison in *in vivo* mouse experiments, a two- tailed, unpaired Student's t-test. For multiple comparisons, a one-way analysis of variance (ANOVA) with a Bonferroni post-test correction was used. For survival analysis, MantelCox. For analysis of small

antigen-specific events (TREC monitoring and intercellular telomere transfer), an analysis of variance with F test was used. Similar statistic assessment was described previously[1,2,12]. Error bars indicate SEM throughout.

Table 1. List of unconjugated antibodies

Antibody	Supplier	Clone	Catalogue number
P53 Rabbit pAb	Cell Signaling	/	9282
p-Ampk α-Rabbit mAb	Cell Signaling	40H9	2535S
P-p38 MAPK - Rabbit mAb	Cell Signaling	D3F9	4511S
P-SAPK/JNK Rabbit mAb	Cell Signaling	81E11	4668S
SESN1 Rabbit pAb	Gene Tex	/	GTX118141
SESN2 Rabbit pAb	Gene Tex	/	GTX116925
SESN3 Rabbit pAb	Gene Tex	/	GTX112277
Histone H3 Rabbit pAb	GIANNI Srl	/	AMab1791
Anti-rabbit IgG, HRPlinked Antibody	Cell Signaling	/	7074S
WDR59 Rabbit mAb	Cell Signaling	D4Z7A	53385S

MIOS Rabbit mAb	Cell Signaling	D12C6	13557S
p-mTOR Rabbit mAb	Cell Signaling	D9C2	5536S

1626

JNK Rabbit pAb	Cell Signaling	/	9252T
H2B Rabbit pAb	Cell Signaling	V119	8135
AMPK total pAb	Cell Signaling	/	2532S
P38 total mAb	Cell Signaling	D13E1	8690S
ERK total mAb	Cell Signaling	137F5	4695T
Anti-FLAG pAb	GeneTex	/	GTX115043
Anti-Myc mAb	GeneTex	/	GTX29106
p-ERK Rabbit mAb	Cell Signaling	D13.14.4e	4370S
GAPDH Rabbit mAb	Cell Signaling	D16h11	5174S
anti-ubiquitinylated proteins mAb	EMD Millipore	FK2	04-263
Rag1 Rabbit mAb	Cell Signaling	D36B3	3968S
Rag2 Rabbit pAb	Invitrogen	XJ3737974B	PA5-88580
α-CD3 Ab	Invitrogen	OKT3	14-0037-82

Acetyl-Histone H3 Rabbit mAb	Cell Signaling	D5EA	8173
5-Methylcytosine Rabbit mAb	Cell Signaling	D3S2Z	28692
HDAC1 Rabbit mAb	Cell Signaling	D5C6U	34589
β -Galactosidase	Cell Signaling	E2U2I	27198
P-16	Cell Signaling	E6N8P	18769
β -Catenin	Cell Signaling	D10A8	8480
KLRG1-biotin	Miltenyi	REA261	130-124-424
p-LCK (Y394) Mouse mAB	R&D Systems	755103	MAB7500
P21 Rabbit mAb	Cell Signaling	12D1	5487
Cyclin D1 Mouse mAB	BD Biosciences	DCS-6	556470

Table 2. List of fluorescent antibodies

Antibody	Supplier	Clone	Catalog number
Anti-human antibodies			
CD3 FITC	Miltenyi	REA613	130-113-138
CD3 PE	Miltenyi	REA613	130-113-139
CD4 Alexa fluor 700	BioLegend	SK3	344622
CD4 FITC	Miltenyi	REA623	130-113-229
CD8 VioBlue	Miltenyi	REA734	130-110-683
CD4 APC-Vio 770	Miltenyi	M-T321	130-100-357
CD27 APC-Vio 770	Miltenyi	REA499	130-113-637
CD27 PerCP-Vio 700	Miltenyi	REA499	130-120-037
CD28 PE	Miltenyi	REA612	130-123-782
CD28 PE-Vio 770	Miltenyi	15E8	130-104-222
CD28 APC	Miltenyi	REA612	130-118-343
CD28 APC-Vio 770	Miltenyi	REA612	130-116-506
CD28 PerCP/Cy5.5	BioLegend	CD28.2	302922
CD45RA BV510	BioLegend	HI100	304142
CD62L PE-Vio 770	Miltenyi	145/15	130-113-621

CD95 FITC	Miltenyi	REA738	130-113-003
CD127 APC/Fire 750	BioLegend	A019D5	351350
TCF1 PE-Cy7	CellSignaling	C63D9	90511S
IFNg APC	Miltenyi	REA600	130-114-021
TCR Vα7.2	Biolegend	3C10	351702
TCR Vβ8 BV421	BDBiosciences	JR2	742412
TCR Vβ7.1 FITC	Miltenyi	REA87	130-114-347
TCR Vβ17 Biotin	Miltenyi	REA915	130-115-345
TCR Vβ2 FITC	Miltenyi	/	130-131-970

1634

TCR Vβ14 Biotin	Miltenyi	REA557	130-108-803
TCR Vβ16 FITC	Miltenyi	REA553	130-108-770
Streptavidin PerCp-Vio700	Miltenyi	/	130-106-795

Phospho-p38 (T180/Y182) Alexa Fluor 488	Cell Signaling	3D7	41768S
Sestrin2 Alexa Fluor 647	Abcam	/	Ab225258
Anti-Mouse antibodies			
Donkey anti-Rabbit IgG Alexa Fluor Plus 647	Invitrogen	/	A-32795
Goat anti-Mouse IgG Alexa Fluor 405	Invitrogen	/	A-31553
Donkey anti-Mouse IgG Alexa Fluor 647	Invitrogen	/	A-31573
Goat anti-Rabbit IgG Alexa Fluor 594	Invitrogen	/	A-11012
CD4 PerCP5.5	BioLegend	RM4-5	100540
CD4 Alexa Fluor 700	BioLegend	RM4-5	557956
CD8 FITC	BioLegend	5H10-1	100804
CD44 APC-Vio 770	Miltenyi	REA664	130-118-695

CD44 BV510	BioLegend	IM7	103043
CD62L PE-Vio 770	Miltenyi	REA828	130-112-649
CD62L APC-Vio 770	Miltenyi	REA828	130-112-839
CD95 FITC	Miltenyi	REA453	130-122-950
Sca-1 PE-Vio 770	Miltenyi	/	130-106-258
IFN-g PE	Miltenyi	REA638	130-117-352
Sestrin2 Alexa Fluor 647	Abcam	/	Ab225258
TCRVβ12 PerCP5.5	Tonbo Biosciences	H57-597	C5961032420653
TCRVα8.3 FITC	BioLegend	B21.14	127705
CD20 PE	Miltenyi	REA294	130-124-435
CD19 APC	Biolegend	1D3/CD19	152409
CD138 Pe-Vio770	Miltenyi	REA104	130-123-883
B220 APC-750	Miltenyi	RA3-6B2	130-102-818
GL7 Pacific Blue	BioLegend	/	144614

IgG FITC	Miltenyi	X-56	130-120-732
CD38 PerCpVio 700	Miltenyi	REA616	130-128-224
TBET PE	Miltenyi	REA102	130-121-340
IFN FITC	Miltenyi	REA638	130-117-780
PD-1 APC	Biolegend	RMP1-30	109111
CXCR5 APC-A750	Biolegend	L138D7	145533

/", indicates polyclonal antibodies

References

1. Lanna, A., Henson, S. M., Escors, D. & Akbar, A. N. The kinase p38 activated by the metabolic regulator AMPK and scaffold TAB1 drives the senescence of human T cells. *Nat Immunol* **15**, 965–972 (2014).
2. Lanna, A. *et al.* A sestrin-dependent Erk-Jnk-p38 MAPK activation complex inhibits immunity during aging. *Nat Immunol* **18**, 354–363 (2017).
3. Eble, J. A. (2018). Titration elisa as a method to determine the dissociation constant of receptor ligand interaction. *Journal of Visualized Experiments* **132**, 57334.
4. Robins, H. S. et al. Comprehensive assessment of T-cell receptor β-chain diversity in αβ T cells. *Blood* **114**, 4099-4107 (2009).
5. Andrews, A. & Bobo, L. (2010). Performance Measurement and Assessment Using Dartfish Software. in Proceedings of E-Learn: World Conference on E-Learning in Corporate, Government, Healthcare, and Higher Education 407–408. 10.4236/ib.2023.151003.
6. Bolotin, D. A. et al. MiXCR: software for comprehensive adaptive immunity profiling. *Nat Methods* **12**, 380–381 (2015).
7. R Core Team. R: A language and environment for statistical computing. (R Foundation for Statistical Computing, 2022).
8. Sidhom, J.-W., Larman, H.B., Pardoll, D.M., and Baras, A.S. DeepTCR is a deep learning framework for revealing sequence concepts within T-cell repertoires. *Nature Communications* **12** (2020).
9. Pizzolla, A. et al. Influenza-specific lung-resident memory T cells are proliferative and polyfunctional and maintain diverse TCR profiles. *J Clin Invest* **128**, 721-733 (2018).
10. Reiss, S. et al. Comparative analysis of activation induced marker (AIM) assays for sensitive identification of antigen-specific CD4 T cells. *PLOS One* **12**, e0186998 (2017).
11. Poloni, C., Schonhofer, C., Ivison, S., Levings, M. K., Steiner T. S. & Cook, L. T cell activation–induced marker assays in health and disease. *Immunol Cell Biol* **101**, 491– 503. (2023).

12. Lanna A *et al.* An intercellular transfer of telomeres rescues T cells from senescence and promotes long-term immunological memory. *Nat Cell Biol* **24**, 1461–1474 (2022).

Figures

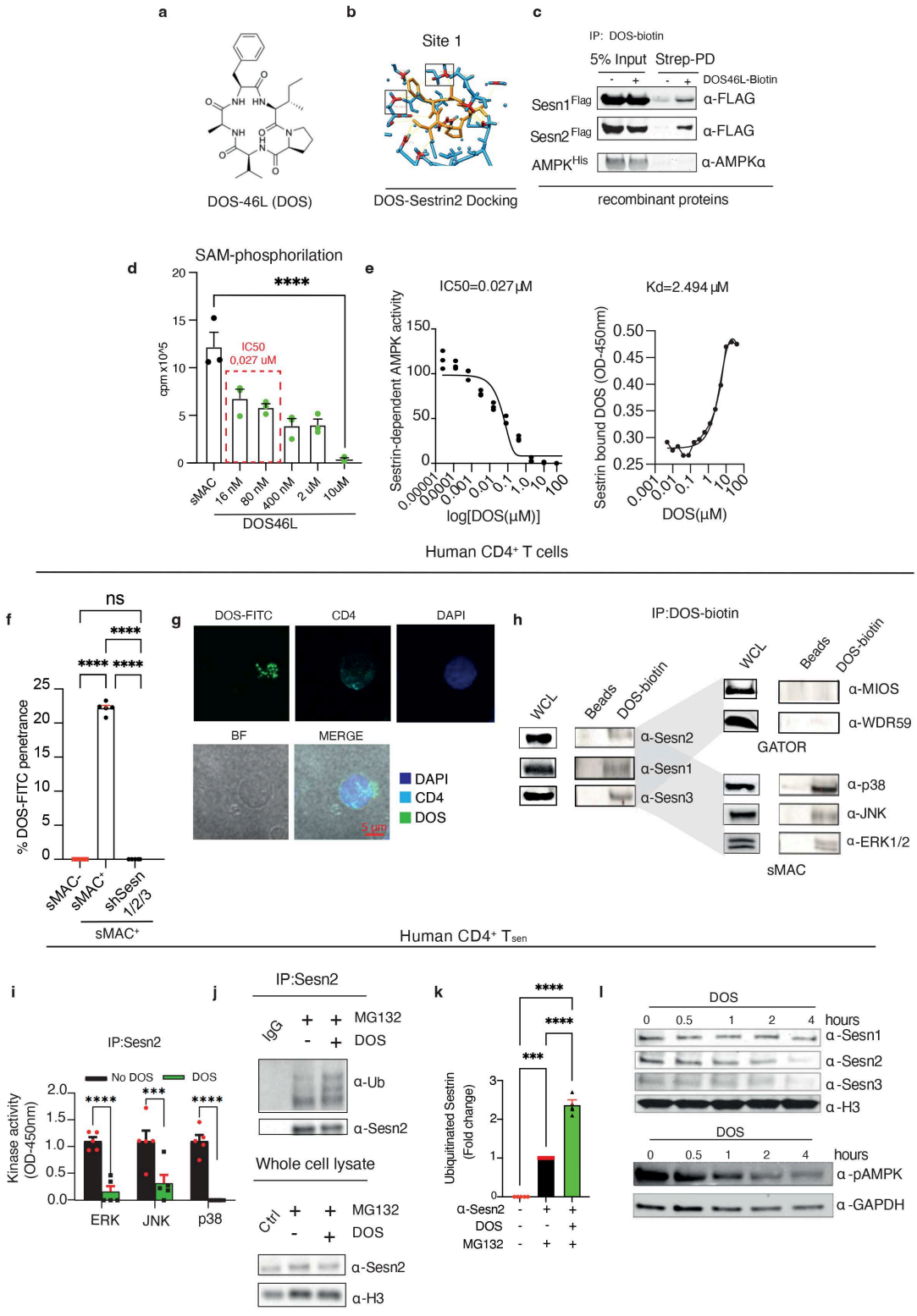

Figure 1

Discovery of DOS a, Molecular structure of the lead compound DOS46L (hereafter, DOS). b, DOS binding site to Sestrin 2 predicted by AutoDock Vina and AlphaFold algorithms. c, Co-Immunoprecipitation of biotinylated DOS46L (DOS; used at 10μM, throughout) followed by recombinant tagged protein detection,

as indicated. d, Recombinant sMAC activity investigated by liquid scintillation. Cpm, counts per minutes. e, Half maximal inhibitory concentration (IC50) of DOS against recombinant 385 sestrin-AMPK complexes by in vitro kinase assays with SAMS peptides and ADP-glo kinase assessment (left); equilibrium dissociation constant (Kd) of sestrin bound biotinylated DOS assessed by ELISA with streptavidin antibodies (right). f, Quantification of selective DOS penetration in sMAC negative and sMAC positive primary human CD4+ T cells by flow cytometry, 30 minutes after DOS treatment (n = 7 donors). g, Individual channels of representative confocal imaging (n = 3 donors) of DOS (green) uptake in human CD4+ T cells. Scale bar, 5 μm. h, Co-Immunoprecipitation (IP, hereafter) of biotinylated DOS from human CD4+ T cell extracts after overnight treatment. Presence or absence of sestrin, p38, JNK, ERK (sMAC) or MIOS and WDR59 (GATOR) was confirmed by western blot in the IP. Whole cell lysates (WCL) controls are shown (same extracts; run in parallel). i, ERK, JNK and p38 MAPK kinase activity (autophosphorylation) among Tsen sestrin 2 immunoprecipitates (sMACs) in the presence or in the absence of DOS for 30 minutes (n = 5 donors). Kinase activity was detected by ELISA assays. j, Human Tsen were pre-treated with the proteasomal inhibitor MG132 (1μM) for 30 minutes followed by addition of DOS for 2 hours. Controls were not treated with DOS. Total lysates and sestrin 2 immunoprecipitates were then analysed by immunoblotting of ubiquitin and sestrin 2. H3, whole cell lysate control. k, Pooled ubiquitination data (n = 5 donors) for experiments as in (i). Data are shown as fold change to the untreated control (NO DOS, in the presence of MG132), set as 1. l, Time dependent assessment of sestrin expression (1, 2 and 3) by DOS in human Tsen (top) and AMPK phosphorylation in the same cells assessed by western blotting (bottom). Representative of 6 donors. In e, f, j, k, one-way Anova with Bonferroni postcorrection for multiple comparisons was performed. **P<0,01; ***P<0,001; ****P<0,0001. Error bars indicate SEM.

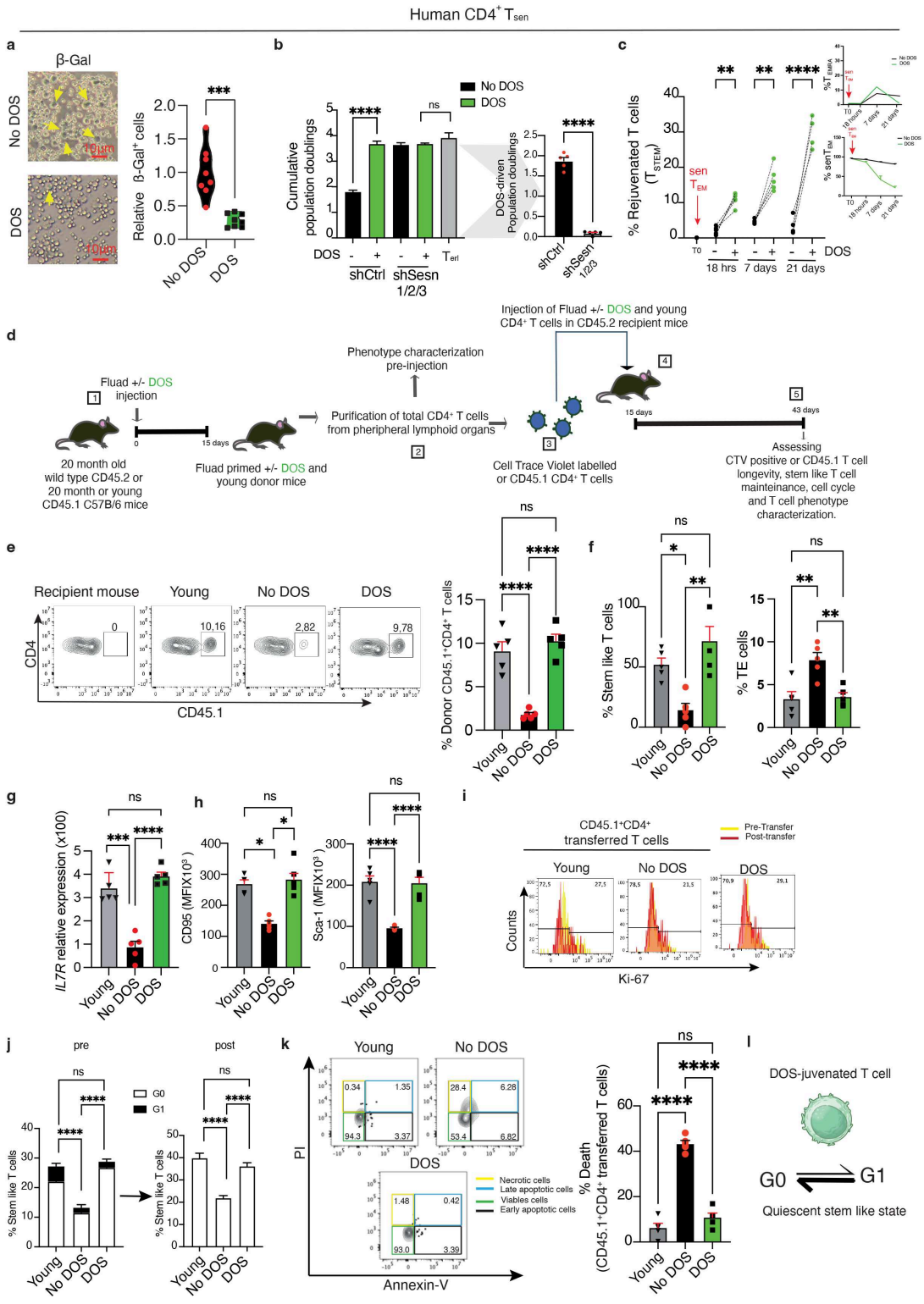

Figure 2

DOS-driven T cell reprograming a, Senescence-associated b-galactosidase expression in DOS-treated (DOS-juvenated) or untreated Tsen. Cells were purified and cultured for one week in the presence of anti-CD3 (0.5 µg/mL) and rhIL2 (5 ng/mL), then stained to detect β-galactosidase activity. Representative image on the inverted phasecontrast microscope (left) and relative quantification (right, n = 8 donors). b, Population doublings of human Tsen (transduced with irrelevant scramble) and sestrin 411 null CD4+

Tsen (transduced by triple lentiviral depletion of sestrins) and cultured as in (a ,left). Donor-matched CD27+ CD28+ CD4+ T cells (herafter, Terl) were cultured in parallel but activated with anti-CD3 and anti-CD28 (n = 5 donors). Cells were cultured over two weeks with restimulation every 7 days. DOS-driven population doublings (right) were calculated as delta between DOS treated and DOS untreated T cells, with or without depletion of sestrins. c, DOS-juvenation of human CD4+ T cells. Terminally differentiated effector memory CD45RA- CD28- CD27- CD4+ T cells (hereafter, senescent TEM) were purified and cultured over 20 days, as in (a) At day 1 (18 hours), 7, and 21 cell phenotypes were assessed by flow cytometry. Quantifications of rejuvenated stem like (CD28+ CD45RA+ CCR7+ CD95+ CD62L+ TCF1+) among human CD4+ T cells are shown (left; n = 5 donors). Decay of senescent TEM and CD28- CD27- CD45RA+ CD4+ T cells (hereafter, senescent TEMRA) undergoing rejuvenation is shown (right). d, Adoptive transfer of DOS-juvenated T cells, experimental design. Donor T cells were derived from twenty-month-old mice 15 days after Fluad vaccination with or without DOS treatment (0.1 mg/Kg throughout), labeled with Cell Trace Violet (CTV) dye or congenic CD45.1 tracking, then transferred into young naïve CD45.2 recipients (3 months). In parallel, young mice (3 months) were used as young donor control. Recipient animals were rested for 28 days, then analyzed for donor T cell persistence and maintenance of stem phenotype after transfer. e, Maintenance of donor DOS-juvenated CD45.1 CD4+ T cells, their aged-matched controls, and that of young donor T cells, 28 days after transfer (day 43) in recipient mouse lymph nodes. Representative flow cytometry plots and poled data (n = 5 mice per group) are shown. f, Assessment of stem like transferred T cells (among CD45.1 CD44- CD62L+ CD95+ CD4+ T cells) and terminally differentiated cells (TE, among CD45.1 CD44- CD62L- CD4+ T cells) following adoptive transfer as in (d) (n = 5 mice per group). g, IL7R gene expression and (h) CD95 and Sca-1 mean fluorescent intensity (MFI; throughout) in stem cells derived from CD4+ CD45.1+ transferred stem T cells among lymph nodes of recipient CD45.2 mice, 28 days after transfer (n = 5 mice per group). i, Representative plots of CD45.1 transferred cells in quiescent state before and after transfer assessed by cycle related intra-nuclear Ki67 staining. Representative of n = 5 mice per group. j, G1 (Ki67+) to G0 (Ki67-) transition in stem like CD45.1 CD4+ T cells 437 before and after adoptive transfer as indicated (n = 5 mice per group). k, Assessment of T cell longevity following DOS439 juvenation. Cells from lymph nodes were stained using the Annexin-PI Apoptosis detection Kit 28 days after transfer. Representative FACS plot (Left) and quantification of dead CD45.1+ CD4+ transferred T cells (Right). Data are from n = 4 mice per group. l, DOS-juvenated T cell maintenance, in vivo model. In a, b (right) two tailed paired T test was used. In b (left), c, e-h, j k one-way Anova with Bonferroni post-correction for multiple comparisons was used, *p<0,05, **P<0,01; ***P<0,001; ****P<0,0001. Error bars indicate SEM.

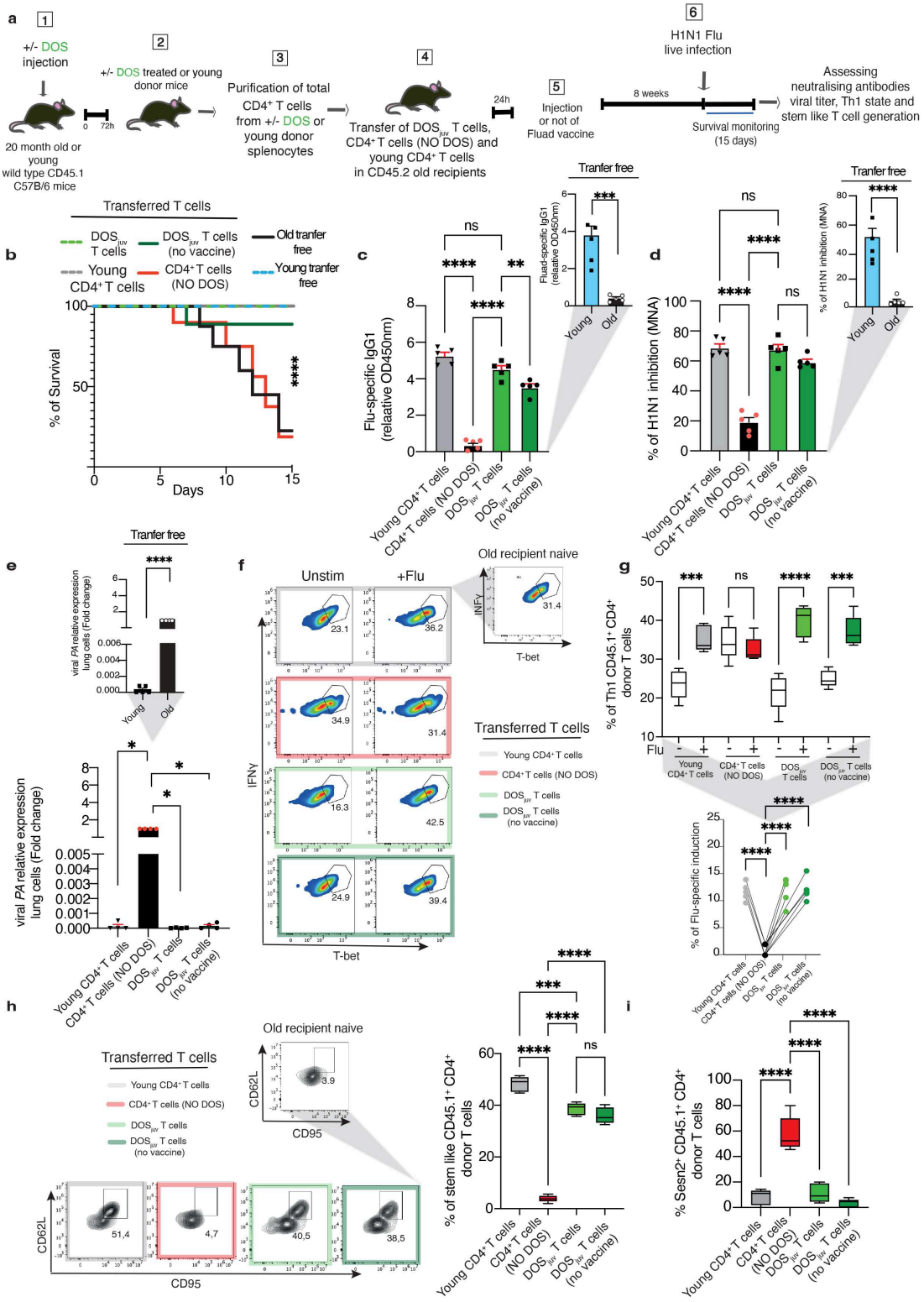

Figure 3

Reprogramed T cells possess prophylactic functions even without vaccination a, Adoptive transfer of DOS-juvenated T cells, experimental design. CD45.1+ CD4+ donor T cells were derived from twenty-month-old mice injected with and without DOS (0.1 mg/Kg throughout), then transferred into old naïve CD45.2 recipients (20 months) 72 hours later. In parallel, young (3 month old) naïve CD45.1 mice were used as young CD4+ T cell donor control. Recipient animals were vaccinated, or not, with Fluad the day

after, as indicated. Animals were subjected to a lethal H1N1 flu viral infection 8 weeks after transfer, and culled within 15 days of infection. Vaccinated young and old mice were also assessed, to determine background responses. b, Survival of mice, Fluad vaccinated, or not, and then challenged with lethal H1N1 infection as in (a). Data are from n = 5 mice per group. c, Fluad-specific IgG production in the same animals subjected to H1N1 infection. Data are from n = 5 mice per group. Transfer free vaccinated recipients are shown (top right; throughout). d, Neutralization properties of Flu-specific IgGs from recipient mice as indicated were assessed upon overnight H1N1 infection of canine kidney cells (MDCK) in vitro by ELISA with anti-influenza A NP antibody. Data are from n = 5 mice per group. e, Viral polymerase acidic protein (PA) assessment in lungs of the same mice upon H1N1 viral infection as in (a) by qPCR (n=5 mice per group). Data are expressed as fold change to the old, infected control (transferred CD4+ T cells, 462 no DOS), set as 1. f, Representative FACS plots and (g) pooled data of primary antiviral Th1 responses among T-bet+ IFNγ+ CD45.1 donor mouse CD4+ T cells as in (a). Data are from n = 5 mice per group. h, CD44- CD62L+ CD95+ CD4+ T cells (stem-like T cells) in animals subjected or not to CD4+ T cell transfer and then infected in the same experiments as in (a); Old naive recipient examples are shown (n = 5 mice per group). i, The fraction of sestrin expressing donor T cells among adoptively transferred CD45.1+ CD4+ T cells from age-matched (20 months) CD45.2+ recipients, six months after transfer as assessed by flow cytometry (n = 5 mice per group). In c-e, g-i, one-way Anova with Bonferroni post-correction for multiple comparisons was used. In c (Top right), e (Top right), a two tailed paired T test was used. In b Mantel-Cox test was used. *P<0,05; **P<0,01; ***P<0,001; ****P<0,0001. Error bars indicate SEM.

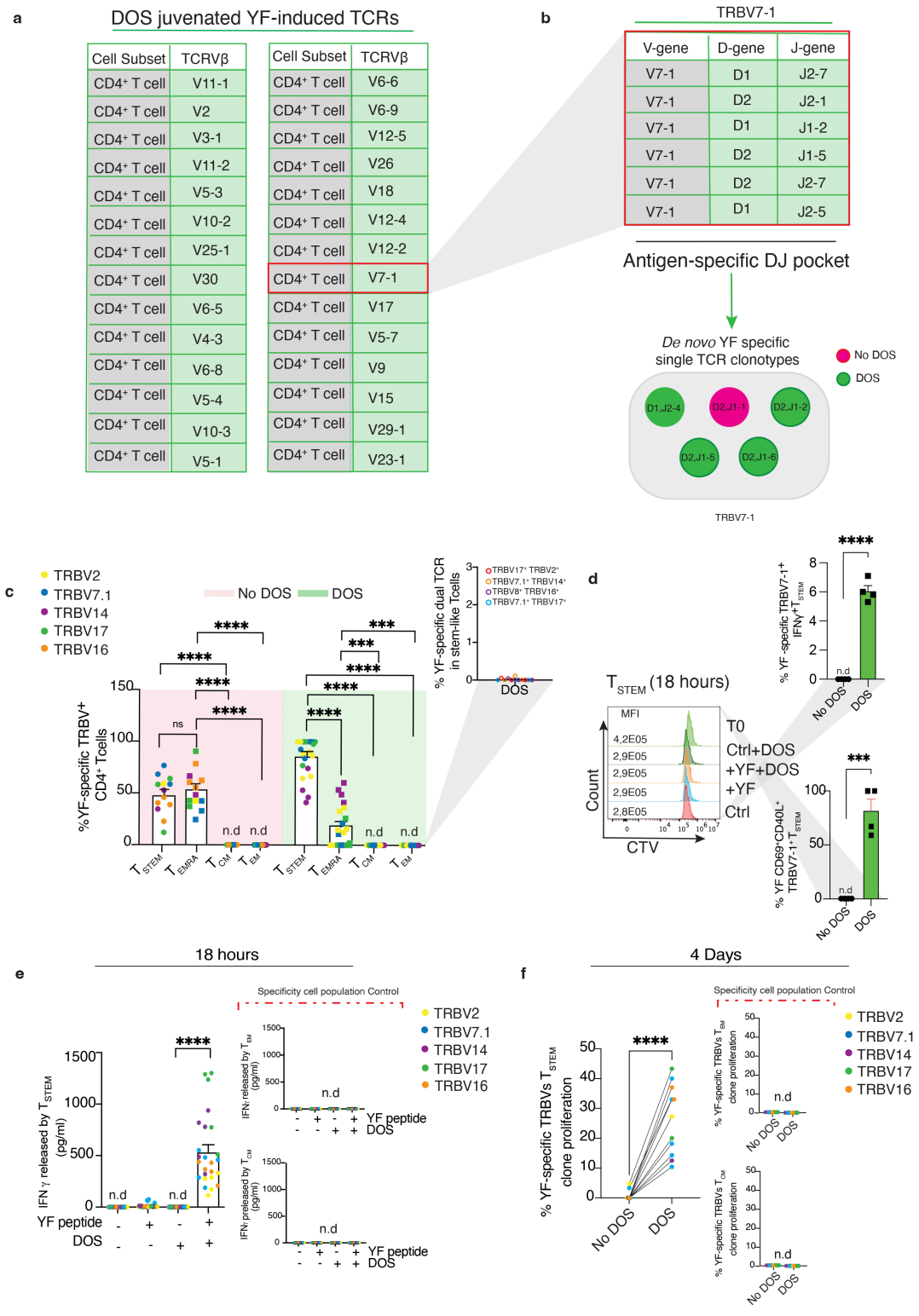

Figure 4

Reprogramed T cells present de novo antigen-specific TCR rearrangements a, Purified human CD4+ T cells and autologous APCs (CD3-depleted PBMCs) were pre-treated or not with DOS or YF peptides (YF) for 4 hours, respectively, then co-cultured for additional 18 hours, in 1:2 ratio. The day after, post-synaptic CD4+ T cell genomic DNA was derived from the conjugates and processed for Next generation sequencing (NGS) of the TCRVB gene. The table shows inductions of T cell receptor Beta Variant (TRBV)

rearrangements (V-DJ recombination) from a single donor upon YF stimulation of DOS-juvenated CD4+ T cells. For experimental details, please see Methods. One representative donor of 4 is shown. Further genomic clonotypes, Extended Data Fig.14. b, Antigen pocket rearrangements among TRBV7-1 variant in T cells derived from the same donor as in (a). Example of single YF-specific TCR clonotypes (among TRBV7-1) that are only seen in T cells exposed to YF-pulsed APCs, with or without DOS (bottom). Note that most antigen pocket rearranging requires presence of DOS, indicating active D-J recombination. c, Single cell presence of YF-specific TRBVs among the different T cell subsets of the 4 donors subjected to NGS. The expression levels of each TRBV were evaluated in individual cells by flow cytometry against the unstimulated background. Each dot is a single TRBV in the single cell flow cytometry assessment. No double TRBVs expressing T cells could be detected (top right). Results from 4 experiments are shown. d, Absence 488 of early YF-specific proliferation (18 hours) of the same stem T cells as shown by CTV tracking. YF-specific TRBV (7.1) clonotypes among the same stem-like T cell clones from 4 different donors, at the same time, is shown (intracellular flow IFN-γ detection; top right). Activation induced markers (AIM) assay of de novo TRBV7-1 YF-specific TSTEM clonotypes (n = 4 donors, bottom right). Antigen free synapses were subtracted. e, IFN-γ release by the indicated TRBV expressing T stem clones after 18-hour YF peptide stimulation and (f) antigen-specific proliferation of the same clones, 4 days after culture as assessed by BrdU incorporation. Cell culture conditions as in (a). Specificity cell population controls (TCM and TEM) are shown. In c, e One-way Anova with Bonferroni post-correction for multiple comparisons was used. In d, f statistical significance was determined by two tailed unpaired student T test. ***P<0,001; ****P<0,0001. Error bars indicate SEM.

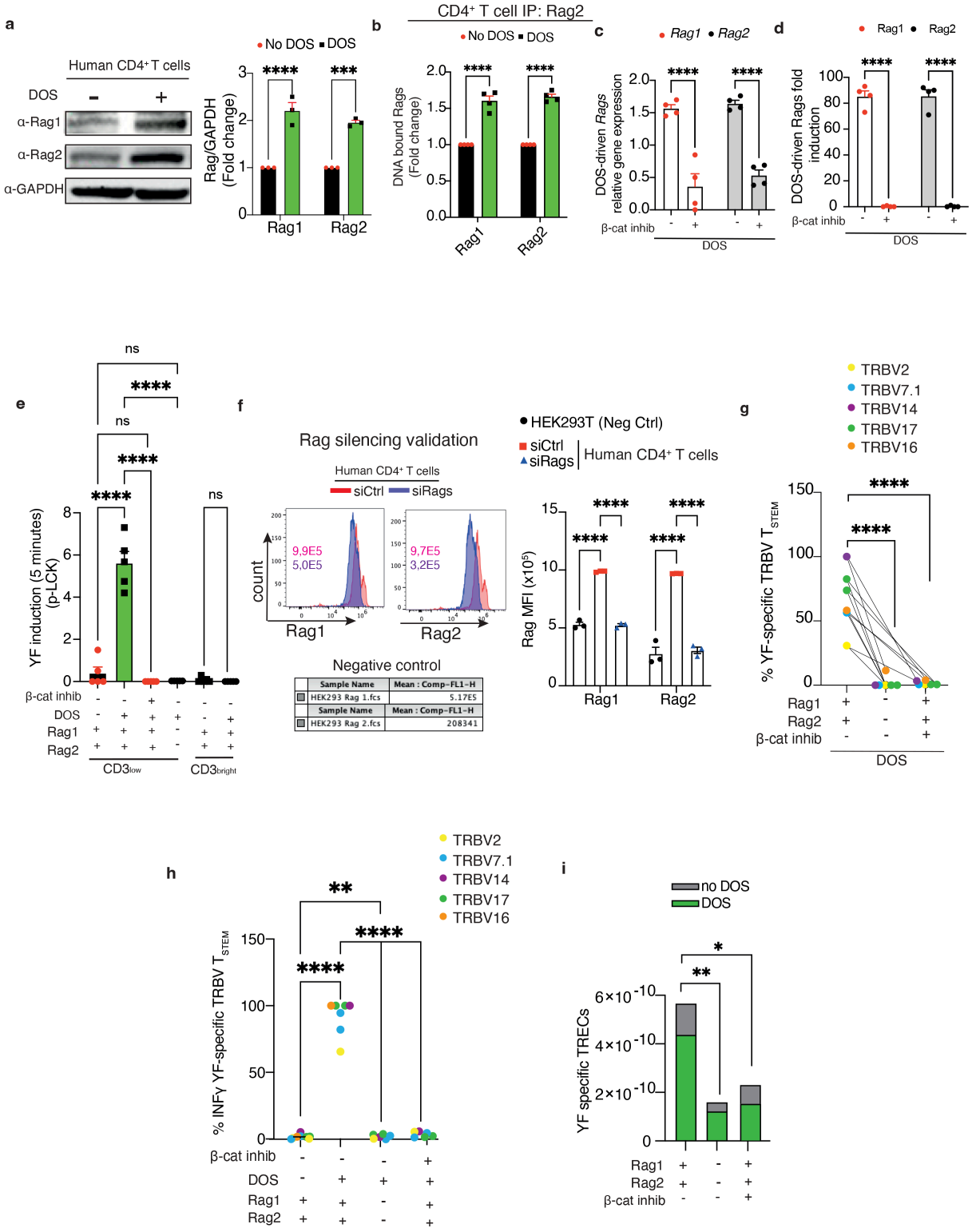

Figure 5

DOS restores Rag function via beta catenin during T cell reprograming a, Representative immunoblots (left) and quantification (right) of Rag protein expression from human CD4+ T cells treated or not with DOS for 4 hours (n = 3 donors). Data are expressed as fold change to the untreated control (no DOS), set as 1. b, Rag 2 proteins were immunoprecipitated from the chromatin of human CD4+ T cells treated as in (a) then followed by ELISA with anti-Rag 1 and 2 antibodies. Data are expressed as fold change to the

untreated control (no DOS), set as 1. c and d, DOS driven Rag induction in the presence or in the absence of beta-catenin inhibition. Senescent TEM were pre-treated or not with the beta catenin inhibitor ICG-001 (10μM, 30') followed by DOS driven reprograming for 4 hours. Rag expression was then investigated by quantitative real time PCR (c) and flow cytometry (d; n = 4 donors). Note absence of DOS-driven Rag generation in the presence of beta catenin blocking. e, YF-specific LCK activation (T394 phosphorylation) among senescent forming TEMRA cultured in the presence or in the absence of beta catenin (ICG-001) or Rag inhibition (Rag- by siRag1/2). Senescent TEM were pre-treated with beta-catenin or Rag inhibition then incubated with DOS for 4 hours, followed by conjugation with autologous YF pulsed APCs for 5 minutes. Results were 514 stratified by relative CD3 expression. Note that only the forming CD3low TEMRA undergo initial YF specific activation (n = 5 donors). f, Representative FACS plot validation (left) and quantification (right; n = 3 donors) of Rag knockdown in human CD4+ T cells. HEK293T cells were used as negative Rag expression control (bottom left). Note that Rag silencing reduces Rag expression to background fluorescence of HEK293 cells naturally lacking Rag proteins, validating known down efficiency. g, Rag deficiency abrogates DOS-driven TCR revisions. Human CD4+ T cells were transfected with siCtrl or siRAG1/siRAG2 for 3 days. The T cells were then treated with or without DOS for 4 hours, in the presence or in the absence of beta-catenin blocking (ICG-001) prior to culture with YF-pulsed or antigen-free APCs for 18 hours. The YF specific DOS-juvenated TCRs derived by background subtraction with no YF peptides are shown (n = 4 donors). h, Effect of Rag protein silencing on the YF-specific IFN-γ production among the indicated stem like T cell clones or on (i), the YF specific TCR rearrangement, assessed by TREC quantification (n = 4 donors). In a-d two tailed paired T test was used. In e-h One-way Anova with Bonferroni correction for multiple comparisons. In f, F test. *P<0,05; **P<0,01; ***P<0,001; ****P<0,0001. Error bars indicate SEM.

Supplementary Files

This is a list of supplementary files associated with this preprint. Click to download.

- NCBED1.pdf
- NCBED2.pdf
- NCBED3.pdf
- NCBED4.pdf
- NCBED5.pdf
- NCBED6.pdf
- NCBED7.pdf
- NCBED8.pdf
- NCBED9.pdf
- NCBED10.pdf
- NCBED11.pdf

- NCBED12.pdf
- NCBED13.pdf
- NCBED14.pdf
- NCBED15.pdf
- NCBED16.pdf